Published in final edited form as:

Curr Biol. 2022 August 08; 32(15): 3245–3260.e5. doi:10.1016/j.cub.2022.06.009.

Selective enhancement of neural coding in V1 underlies fine discrimination learning in tree shrew

Joseph W. Schumacher[1], **Matthew K. McCann**[1,2], **Katherine J. Maximov**[1,3], **David Fitzpatrick**[1,4]

[1.] Functional Architecture and Development of Cerebral Cortex, Max Planck Florida Institute for Neuroscience, 1 Max Planck Way, Jupiter, Florida 33458, USA

[2.] Synapses – Circuits – Plasticity, Max Planck Institute for Biological Intelligence, in foundation, Am Klopferspitz 18, D-82152 Martinsried, Germany*

[3.] Solomon H. Snyder Department of Neuroscience, Johns Hopkins University School of Medicine, 1003 Wood Basic Science Building, 725 N. Wolfe Street, Baltimore, Maryland 21205, USA*.

Summary

Visual discrimination improves with training, a phenomenon that is thought to reflect plastic changes in the responses of neurons in primary visual cortex (V1). However, the identity of the neurons that undergo change, the nature of the changes, and the consequences of these changes for other visual behaviors remain unclear. We used chronic *in vivo* 2-photon calcium imaging to monitor the responses of neurons in V1 of tree shrews learning a Go/No-Go fine orientation discrimination task. We observed increases in neural population measures of discriminability for task-relevant stimuli that correlate with performance, and depend on a select subset of neurons with preferred orientations that include the rewarded stimulus and nearby orientations biased away from the non-rewarded stimulus. Learning is accompanied by selective enhancement in the response of these neurons to the rewarded stimulus that further increases their ability to discriminate the task stimuli. These changes persist outside of the trained task and predict observed enhancement and impairment in performance of other discriminations, providing evidence for selective and persistent learning-induced plasticity in V1 with significant consequences for perception.

eTOC Blurb

[4]Lead contact, correspondence: David.Fitzpatrick@mpfi.org.
*denotes current departments

Author contributions:

JWS and DF designed the study and experiments. JWS performed all surgeries with assistance from MKM and KJM. JWS, MKM, KJM, performed the imaging, optogenetic and behavioral experiments. JWS and MKM analyzed the data. DF provided input on all aspects of the project. JWS and DF wrote the manuscript.

Declaration of interests

The authors declare no competing interests.

Schumacher et al. show that learning fine visual discriminations is accompanied by enhancement in the discrimination capacity of tree shrew V1 neurons. This enhancement results from persistent changes in the tuning properties of a select group of task-relevant neurons that lead to predictable biases in performance of other visual discriminations.

Keywords

visual cortex; perceptual learning; neural coding; tree shrew; neural discrimination

Introduction

Neurons in primary visual cortex (V1) respond selectively to different stimulus features[1], constructing neural representations that reliably encode the visual information necessary to support perception and behavior[2–4]. Visual experience plays a critical role in the early development of these representations[5], and there is considerable evidence that these representations remain plastic in the mature brain, allowing learning to enhance the discrimination of sensory stimuli necessary to perform novel tasks[6]. This process has been explored through visual perceptual learning paradigms in which behavioral training with visual stimuli improves discrimination or detection performance[3, 4, 7–11]. Perceptual learning is thought to result from persistent changes in the activity of a subset of cortical neurons whose properties are well-suited to discrimination enhancement [11, 12], but the cortical regions undergoing change and the nature of the changes remain debated[13, 14]. Moreover, in those studies where V1 response properties such as orientation selectivity [4, 11], direction tuning[8], contrast sensitivity[10], and contour detection[15, 16] have undergone change with perceptual learning, the full impact of these changes on the neural representation of stimulus features under active and passive viewing conditions remains unclear.

To address these issues we employed a 2-photon *in vivo* imaging paradigm that allowed us to longitudinally track the responses of large populations of V1 neurons through an orientation-discrimination learning paradigm in the tree shrew, a close relative of primates with a visual cortex that exhibits a highly organized functional architecture[17–19]. With training, animals were able to improve their ability to discriminate the orientation of rewarded and non-rewarded stimuli in a V1-dependent Go/No-Go orientation discrimination task. Enhanced performance was accompanied by changes in the responses of individual V1 neurons that improved the population's ability to discriminate rewarded and non-rewarded stimuli. These changes were restricted to a select subset of neurons with pre-training tuning properties well-suited for identifying the presence of the rewarded stimulus, and the selective enhancement in their responses to the rewarded stimulus further increased their ability to discriminate the task-relevant stimuli. Similar, but weaker, learning-related changes were observed under passive conditions, revealing changes in single neuron response gain, preferred orientation, and tuning curve symmetry that contribute to the enhanced neural discrimination. Moreover, the persistence of these changes outside the behavioral task predicts enhancements and impairments in the discrimination of other orientations that we observed in subsequent behavioral tasks. These results suggest that perceptual learning involves persistent changes in the response properties of a task-relevant subset of

V1 neurons, modifying the representation of visual stimuli in a way that enhances task performance at the expense of other related discriminations.

Results

Tree shrews learn to perform a V1-dependent, fine orientation discrimination task.

To assess the role of V1 in learning and performing a perceptual discrimination, we trained tree shrews to perform a simple Go/No-Go orientation discrimination task (Figure 1A). Tree shrews self-initiated individual trials by licking their reward port, and, following a variable delay, were presented with a 500ms static oriented grating. If the orientation of the grating matched the assigned rewarded orientation (S+), licking during the subsequent 1.5 second response period would result in a liquid reward (hit), while failure to lick (miss) would result in a timeout (see STAR Methods). If the grating orientation did not match the S+, a lick response (false alarm, FA) resulted in a timeout, while withholding a response was considered a correct rejection (CR) of the non-rewarded orientation (S−). There is considerable variation in the implementation of Go/No-Go behavioral tasks for behavioral and neurophysiological studies [4, 7, 20–25], but the typical Go/No-Go task has the limitation that non-responses are somewhat ambiguous since they can result from correct task performance or other factors such as attentional lapses or fluctuating motivational factors[7]. Furthermore the timing and ratio of delivery of S+ and S− stimuli can systematically alter task engagement and performance biases[20]. To incentivize sustained task engagement, especially throughout No Go trials, S− CRs were “rewarded” with a subsequent S+ and response period (Figure 1A). Because these additional presentations had a 100% probability of being the S+, hit responses could be driven by a strategy independent of visual discrimination, and for this reason they were excluded from overall performance calculations. Finally, to provide a disincentive for licking during the stimulus presentation, lick responses that occurred before stimulus offset resulted in aborted trials regardless of trial type (S+ or S−).

To become familiar with the testing apparatus and learn the reward contingencies of the task, animals were first trained to perform coarse discriminations (>=45 degrees). Characteristic learning behavior was observed as a refinement of licking response times (Figure 1B). On day 1 (Figure 1B, left), the animal learned to time licking responses after the 500ms stimulus presentation, but responds on both S+ (black dots) and S− (red dots) trials, and responses on these trials were distributed over the course of about 1 second (lick timing histograms, Figure 1B, bottom). Following 7 days of training (Figure 1B, right), the timing of Go responses was more locked to stimulus onset, and the fraction of responses on No Go trials was substantially reduced, indicating improved discrimination. Tree shrews (n=11) typically reached criterion performance levels (d’>=1) for coarse discrimination in under 7 training sessions (Figure 1C, left; mean days to criterion = 6.17 +/− 2.92 SD).

To establish the psychophysical limits of behavioral performance under our system, a subset of animals (n=7) were trained to discriminate multiple S− stimuli with offsets from the S+ at increments of 10, 22.5, and 45 degrees. Peak performance at each offset (Figure 1D) yields individual psychometric curves that demonstrate a group performance breakdown at discriminations of 10 degrees. Animals reliably have high Go rates for S+ stimuli (offset

= 0 degrees), and low Go rates for S− offsets from target by 22.5 degrees or higher, but have highly variable performance with 10 degree discriminations, with shrews less able to suppress Go responses. For subsequent experiments, 22.5 degree discriminations were considered “fine” discriminations, because they posed a greater challenge than coarse discriminations of 45 degree discriminations and above, but a majority of animals were able to reach criterion performance at this level of difficulty.

Animals used for the imaging experiments (n = 5) and additional behaviorally trained animals (n = 4) mastered the coarse discrimination task, and were then introduced to an S− stimulus that was offset by 22.5 degrees from the previously trained S+ target stimulus (Figure 1E; n = 9; days to criterion = 7.44 +/− 3.0 SD). The time to criterion performance did not differ significantly between coarse and fine discrimination periods ($p>0.4$, two-sample t-test), suggesting that while the coarse task instructed the animal to use the apparatus and learn a set of reward contingencies, there remains a general lack of transference of perceptual skill from coarse to fine discrimination learning. Because the novel 22.5 degree S− is equidistant from the original S− and original S+, it likely takes time for the shrew to perceptually group this stimulus into the correct response category (No Go), and perceptually differentiate it from the other category (Go).

Before examining the responses of V1 neurons during the discrimination task, we thought it was important to confirm that V1 activity contributes to task performance. Early behavioral work in tree shrews found that visual discrimination could be retained or quickly reacquired in tree shrews with full ablations of striate cortex[26], possibly through the preservation of the tectothalamocortical pathway[27]. To address this issue, in animals that had learned the discrimination, we transiently suppressed V1 activity bilaterally during presentations of the visual stimulus, interleaving trials with or without optogenetic activation of inhibitory interneurons that virally expressed channelrhodopsin[28, 29] (mdlx.ChR2). In separate experiments we validated the suppression of V1 responses with this approach, demonstrating that blue light stimulation induces hyperpolarization of putative pyramidal cells and depolarization accompanied by fast-spiking activity in a putative interneuron (Figure 1F, see STAR methods). We also titrated the intensity of blue light stimulation to arrive at an intensity sufficient to achieve maximal suppression of spike rates (8 mW/mm^2; Figure 1G,H). Consistent with the contribution of V1 activity to task performance, in two tree shrews with bilateral mdlx.ChR2 expression, discrimination was significantly impaired on the trials with optogenetic stimulation (Figure 1I; $p<0.01$ Wilcoxon signed rank test). To control for the possibility that these effects were due to the presence of blue light stimulation during the trial rather than silencing of V1 neurons, we performed the same experiments before the animals received injections of the AAV delivering the ChR2 transgene. The blue light stimulation alone did not significantly impair behavioral performance (paired t-test in two animals, $p = 0.38$ and $p = 0.72$) (Figure S1A).

While discrimination performance was impaired by silencing V1 neurons, it was not eliminated, and this is likely due to the fact that optogenetic manipulation of V1 responses was spatially limited to the region within and surrounding the viral injection site. By mapping the retinotopy of the cortical region within the cranial windows using intrinsic signal imaging, we estimate an area roughly 24 degrees in elevation and 20 degrees in

azimuth near the center of gaze would have been impacted by the optogenetic manipulation (Figure S1B). Thus, the residual discrimination performance in these experiments is likely to reflect contributions from intact areas of V1. Overall, these experiments support the view that visually driven patterns of activity in V1 contribute to the performance of this discrimination.

V1 neural populations improve fine discrimination performance with learning.

We then asked if the learning of fine orientation discrimination with the Go/No-Go task is accompanied by changes in the response properties of V1 neurons that could facilitate task performance. We chronically imaged neural activity in populations of tree shrew V1 layer 2/3 neurons with two-photon calcium imaging of the genetically encoded calcium indicator GCaMP6s[30], which we expressed via microinjections of AAV vectors (see STAR Methods). This enabled us to measure responses to S+ and S− stimuli during behavioral performance at multiple time points relative to criterion fine discrimination performance (Figure 2A). Alignment of the chronically imaged field of view was facilitated by anatomical landmarks such as neuronal somata, blood vessels, and cortical depth relative to the imaging window coverglass (Figure 2A, left). Representative example neurons show that raw responsiveness remains relatively stable across learning time points, with notable changes (Figure 2A,B). Cell 1 is an example of an S+ responsive cell that gains responsiveness over the course of fine discrimination learning, while Cell 2 is an example of an S− responsive cell that has diminished responsiveness across time points (Figure 2B; for additional examples see Figure S2A).

In order to derive a measure of population neural discriminability—i.e., how well the S+ and S− stimuli can be discriminated based on the activity patterns of many V1 neurons, we turned to a dimensionality reduction approach used by previous population coding studies[31, 32]. Figure 2C schematizes this process, where each point represents an individual trial's population response in n-dimensional population space (n = number of cells), and is color coded by the orientation presented on that trial (Figure 2C, top). To determine the neural population's capacity to discriminate these clusters of population responses, we calculate the separability of each cluster from one another by projecting each point in n-dimensional space onto the one-dimensional vector between the mean population responses of two stimuli. Population responses to individual stimuli form distributions of values along this separability dimension (Figure 2C, bottom). These distributions are then the basis for quantifying neural population discrimination performance ($d'_{pop.}$) using a standard separation index (see STAR Methods). In the pre-learning phase, the population responses to the S+ and fine (22.5 degree offset) S− for these animals are highly overlapping suggesting that the naïve V1 population responses provide less of a basis for reliable fine discrimination. Following behavioral training (Figure 2D, right), enhanced behavioral performance was accompanied by significant increases in the neural discriminability (Paired t-test, $p < 0.05$) of these stimuli based on V1 responses within the population of chronically tracked neurons (Figures 2E, S2B).

Single cell discrimination improvements are orientation specific and linked to reward associations.

To better understand changes in the population response of V1 neurons that contribute to enhanced discrimination, we started by characterizing the patterns of activity evoked by the S+ and S− stimuli prior to learning the discrimination. Tree shrew V1 has a well-organized modular architecture for orientation preference[18, 19], and this was clearly evident in awake head-fixed animals with passive presentation of grating stimuli (Figure 3A). As expected, presentation of the S+ (Figure 3B, left) and S− (Figure 3B, right) stimuli during the behavioral paradigm resulted in robust modular responses that were distinct, but highly overlapping (outlined in Figure 3A), reflecting the orderly progression of orientation preference and the breadth of tuning exhibited by individual layer 2/3 neurons. Well-tuned neurons' median tuning curve (full width at half max) was 55 degrees +/− 13.98 SD (see STAR Methods), consistent with previous observations in both tree shrew[33] and primate[34, 35]. Thus, prior to learning, individual V1 neurons that are activated by the S+ and S− stimuli differ in the degree to which their activity patterns can contribute to the discrimination of the two stimuli, depending on the relation of their tuning curve to the S+ and S− orientations [11, 36].

To derive a population response profile that represents the distribution of neural activity evoked by S+ and S− stimuli as a function of a neuron's orientation preference, passive presentations of the full range of orientations were used to compute the pre-learning preferred orientation for each neuron in our longitudinally tracked sample (see STAR Methods). Using this data, cells (n = 377) were pooled across animals (n = 5) and were binned by preferred orientation (orientation axis normalized across animals: 0 degrees = S+, 22.5 degrees = S−), and a moving average (+/− SEM) across orientation bins (10 degree width, 5 degree increments) was computed for single cell responses to the S+ and S− stimulus (Figure 3C) In the pre-learning condition (Figure 3C, left), the peak responses for the S+ and S− stimulus were distributed around neurons with corresponding preferred orientations, but each stimulus evoked responses from neurons with a broad range of preferences, resulting in significant overlap of the two distributions. Following learning (Figure 3C, right) there was a noticeable change in the response to the S+ stimulus, with increases in the responses of neurons with preferred orientations that include the S+ orientation and nearby orientations biased away from the S− orientation. There also appeared to be a modest decrease in the response to the S− stimulus for neurons that prefer the S− and neighboring orientations.

These results suggest that the behavioral increase in discrimination performance is not simply the result of an increase in responses of V1 neurons to the rewarded stimulus, but an increase in response of a select subset of neurons whose tuning is optimal for distinguishing the rewarded stimulus from the distractor. To specifically test the discrimination capability of the population of neurons in our sample, we calculated single cell (S+,S−) discriminability (d'_{sc}; see STAR Methods) using single cell *d*F/F signals on a trial-by-trial basis. Then, by arranging baseline (pre-learning) d'_{sc} by preferred orientation and averaging over bins of 10 degrees, we could evaluate the distribution of d'_{sc} values for both pre- and post-learning conditions. As expected, in the pre-learning condition, the

distribution of d'_{sc} values exhibits two peaks separated by a trough: the lowest d'_{sc} -values are found for neurons with preferences for orientations in between the two stimuli, while higher d'_{sc} -values are found for neurons that prefer orientations displaced away from this region (Figure 3D, left)[11, 36]. Interestingly, post-learning, the discrimination profile of the neural population has a strikingly different appearance with an increase in d'_{sc}, especially for neurons with preferred orientations neighboring the S+, and biased away from the S−. This is accompanied by a modest reduction in d'_{sc} for neurons with preferred orientations near the S−.

To better understand the learning induced changes in single neuron responses that contribute to the increases in the population d', we determined the d'_{sc} values for individual neurons pre- and post-learning and computed the difference ($\Delta d'_{sc}$). Plotting these values according to each cell's pre-learning preferred orientation (Figure 3E, top), we confirmed that individual neurons with the greatest improvements in task discrimination are those with preferred orientations flanking the S+ orientation and displaced away from the S− orientations (S+ flanking neurons). We quantified this further by computing a moving average of all $\Delta d'_{sc}$ within 20 degree bins over 5 degree increments. We found significant improvements in $\Delta d'_{sc}$ for cells with preferred orientations within 35 degrees of the S+ stimulus and shifted away from the S− stimulus, but in no other preferred orientation bins (Figure 3E, bottom; $p<0.05$ Wilcoxon signed-rank test). This analysis also revealed a significant reduction in $\Delta d'_{sc}$ for neurons with preferences near the S− (Figure 3E, bottom; $p<0.05$ Wilcoxon signed-rank test).

While the learning induced enhancement in discrimination is clearly biased to the S+ flanking neurons, the single neuron analysis reveals that there is considerable diversity in the behavior of neurons regardless of preferred orientation. To further probe this diversity at the single cell level, we determined the percentage of neurons in our sample that exhibited significant change in response pre- and post-learning, and characterized the nature of this change (see STAR Methods). In fact, out of all neurons tracked longitudinally (Figure 3F, i.; n =377), only 22% (n = 82) exhibited a significant change in response magnitude, changes that included increases or decreases in response to the S+ or S− and various combinations. But the distribution of the neurons undergoing change and the types of change they exhibited was distinct for S+ and S− flanking neurons (n = 106 and 134, respectively; S− flanking neurons are those with preferred orientations flanking the S− orientation and displaced away from the S+ orientation). Approximately 31% of S+ flanking neurons exhibited significant changes in response, 66% of which exhibited an increase in response to the S+ stimulus (Figure 3F, ii.). In contrast, only 22% of S− flanking neurons underwent significant changes in response with the greatest fraction (51%) decreasing their response to the S−, and only 22% exhibiting increased responses to the S+ stimulus (Figure 3F, iii.). These results indicate that while neurons in V1 undergo heterogeneous learning related changes as a group, orientation specific enhancement of neural discrimination is largely driven by increases in S+ responsiveness. Interestingly, this increase in S+ responsiveness was not accompanied by changes in S+ response reliability (coefficient of variation of dF/F) for neurons tuned within the 35 degree S+ flanking region (Wilcoxon signed rank test, $p>0.1$) or S− flanking region (Wilcoxon signed rank test, $p>0.68$).

We then asked how well these results generalize to individual animals (Figure S3). At the full population level, our sampling of pre-learning preferred orientations is roughly uniform relative to each shrew's task-related orientations (Figure S2D), and in all of the shrews, the pre-learning population response profile for the S+ is displaced away from that of the S− (Figure S3A). However, the pre-learning degree of population overlap, and the relative magnitude of the population response to the S+ and S− differ across animals, with some being roughly equal (Shrew 1,3,4) and others exhibiting a greater response to the S+ (Shrew 2) or the S− (Shrew 5) (Figure S3A, left). Likewise post-learning, the population response profile to the S+ increases in all of the shrews, but the change in the population response to the S-varies across shrews, decreasing (Shrew 4 and 5), increasing (shrew 1 and 3) and remaining relatively constant (shrew 2) (Figure S3A, right). Despite this variation, and consistent with the pooled population analysis, in each animal, learning is associated with an increase in d' for subpopulations of neurons with preferences that flank the S+ orientation and are displaced away from the S− stimulus (Figure S3B,C).

Learning-enhanced neural discrimination persists outside of task performance and is associated with biased changes in orientation tuning

While the training-induced enhancement in neural discriminability can be explained by changes in the response of a select subset of V1 neurons, it leaves open the question of whether this enhancement is context-dependent - only evident during performance of the task - or extends to stimuli presented outside the behavioral paradigm. To probe this issue we examined whether we could detect learning-induced $\Delta d'_{sc}$ of neuronal responses under passive stimulus presentation conditions (Figure 4A). As in the behavioral paradigm, we observed (Figure 4A,B) an overall increase in d'_{sc} that was specific for the S+ flanking neurons ($p<0.05$, Wilcoxon signed-rank test). These results indicate that fine discrimination learning is accompanied by stimulus-specific increases in d'_{sc} that persist outside of the behavioral context in which they arise. Moreover, as seen with population responses recorded during task performance, in all 5 tree shrews, learning was accompanied by enhancement of passive neural discriminability of the S+ and fine S− (Figure S2C; $p < 0.05$ paired t-test).

The consistency of V1 population changes in active and passive contexts suggests that discrimination learning reflects a persistent increase in the discrimination capacity of a subset of V1 neurons whose tuning is well-matched to the task. But, this assumes that the neurons that undergo enhancement in the active condition exhibit enhanced responses in the passive condition.

To further explore the relation between the changes in the active and passive conditions at the single neuron level, we derived the conditional probability of a cell increasing its response to the S+ in the passive condition, given an increase in S+ response in the active condition, and determined whether this was significantly different from a random relationship (Figure S4A,B). A bootstrapped distribution was computed by randomly sampling the individual cellular outcomes of increases in the S+ (S+ increased or didn't increase) in both the active and passive cases, and then computing the conditional probability over 100,000 bootstrap samples. From these distributions, the 95 and 99%

confidence intervals were determined. In all cases, the observed conditional probability fell well beyond the 99% confidence interval, indicating that the number of cells changing their S+ response in both the active and passive condition is significantly greater, to a high degree, than what would be expected with random sampling.

The fact that changes in neural discrimination persist to a large degree in the passive condition made it possible to further characterize the functional changes in response underlying the enhanced discrimination of individual S+ flanking neurons. In principle, the changes in the responses of S+ flanking neurons could reflect uniform increases in gain, shifts in preferred orientation, changes in the shape or symmetry of the tuning curve (Figure 4C), or some combination of these factors. To assess the types of changes that occur with learning, we used measurements of the underlying tuning properties of neurons in the passive viewing condition. We restricted these analyses to neurons with sufficient responsiveness and orientation tuning (tuning curve 1-CV > 0.25, see STAR Methods) in both the pre- and post-learning time points. The percentage of visually responsive neurons was determined to be 69.76% in the pre- and 72.68% in the post-learning conditions, with 66.31% of neurons being significantly responsive across both sessions. A small subset of neurons (6.4%) that were not strongly visually responsive in the pre-learning condition gained responsiveness in the post-learning condition. The post-learning preferred orientations of these neurons were broadly distributed, covered nearly the entire possible range (−80.87 to 77.95 degrees) and were not strongly linked to orientations neighboring the S+. Moreover, the distribution of changes in d’ for these neurons did not significantly increase or decrease (median $\Delta d' = -0.04$; Wilcoxon signed-rank test, $p=0.67$), indicating that the recruitment of these visually responsive neurons did not contribute to increased discrimination performance at the population or behavioral levels.

Neurons with preferred orientations in the S+ flanking region exhibited significant increases in overall response magnitude (Figure 4D, top; $p<0.001$, Wilcoxon signed-rank test), while neurons tuned to the S− flank did not (Figure 4D, bottom; $p>0.2$ Wilcoxon signed-rank test). This is consistent with our finding that S+ flanking neurons had predominant increases in response to the S+ in the active condition (Figure 3F).

We then asked whether S+ or S− flanking neurons underwent shifts in preference or tuning curve shape that would be consistent with improved single cell discrimination. Overall, the pre- and post-learning orientation preferences of the total population of tuned neurons in our sample were highly correlated (Figure S4C). Nevertheless, the subpopulation of neurons with preferred orientations in the S+ flank exhibited a distribution of post-learning preferred orientations that was significantly biased toward the S+ relative to the pre-learning state (Figure 4E, top; positive bias $p<0.001$, Wilcoxon signed rank test). Significant shifts in single cell orientation tuning ($p<0.05$, Watson-Williams test for equal means, see STAR Methods) were observed in 16.67% of these S+ flanking neurons, and while the percentage of S− flanking neurons that exhibited significant shifts was greater (20.41%, $p<0.05$, Watson-Williams test for equal means) these neurons exhibited no significant directional bias in the distribution of pre/post-learning changes of orientation preference ($p>0.05$, Wilcoxon signed-rank test; Figure 4E, bottom).

To determine whether changes in the underlying shape of the orientation tuning curve could also contribute to enhanced neural discrimination in the S+ flanking neurons, we employed a measure of tuning curve asymmetry (Asymmetry Index, see STAR Methods) to compare the values for individual neurons before and after discrimination learning. This metric ranges from −1 to 1 describing whether the shape of the tuning curve is uniform around the preferred orientation, or biased to the left or right respectively. For example, a neuron with a preferred orientation of −40 degrees from the S+ with a positive Asymmetry Index value would respond more vigorously to stimuli in regions of its tuning curve close to the S+, than stimuli with orientations equidistant from its preferred orientation in the opposite direction. We first compared Asymmetry Index values for all visually responsive cells in the S+ and S− flanking regions. S+ flanking neurons exhibited significant positive shifts in their Asymmetry Index with learning (Figure 4F, top; $p<0.001$, Wilcoxon signed-rank test), while S− flanking neurons did not (Figure 4F, bottom; $p=0.154$, Wilcoxon signed-rank test). This suggests that learning is accompanied by biased shifts in the responsiveness of some neurons in the S+ flank that could contribute to their increased capacity to discriminate S+ vs S−.

This led us to wonder whether the magnitude of the learning-related changes in the discriminability of individual neurons in the S+ flank could be related to the magnitude and direction of the changes in tuning properties. Neurons in the S+ flank with high increases in d'_{sc} (delta d'_{sc} >1, or approximately the 95th percentile of changes in d'_{sc}), underwent significantly positive changes in gain (Figure 4G), preferred orientation (Figure 4H), and asymmetry index (Figure 4I; $p<0.01$ Wilcoxon signed-rank test). In contrast, the subpopulation of neurons with changes in $d'_{sc}<1$ did not undergo significant positive or negative changes in Asymmetry Index or preferred orientation, and displayed high variability in the types of functional changes they exhibited (Figures 4H, I). This suggests that underlying changes in the tuning function of neurons that accompany learning are correlated with improvements in the neural discriminability of task relevant stimuli. Interestingly, S+ flanking neurons with changes in $d'_{sc}<1$ did undergo significant increases in excitation gain (Figure 4G; $p<0.05$, Wilcoxon signed-rank test). This indicates that S+ flanking neurons undergo a generalized increase in responsiveness that is not necessarily tied to large improvements in single cell discrimination. Taken together, these results suggest that changes in multiple functional properties contribute to the enhancement of single-cell neural discrimination.

We then asked whether there was any association between initial tuning preference and the degree of change observed in the asymmetry index or preferred orientation within the subpopulation of neurons with high increases in d'_{sc}. We did not observe a significant correlation between initial orientation preference and changes in peak response (Figure 4J; $p > 0.06$, R-squared = 0.17) or changes in preferred orientation (Fig. 4K; $p = 0.18$, R-squared = 0.08): neurons with initial preferences in the S+ flanking region seemed to broadly increase their excitation and shift their orientation preference toward the S+. We did observe a significant correlation between initial orientation preference and the magnitude of change in Asymmetry Index ($p<0.01$, R-squared = 0.39): neurons with initial orientation preferences that were more displaced from the S+ had greater increases in their Asymmetry Index than those with proximal orientation preferences (Figure 4L). Taken together, these results suggest that the enhanced discriminability of the S+ flanking neurons derives from

mechanisms of circuit plasticity that can fundamentally alter the tuning properties of neurons in a task-specific fashion.

Given the presence of a well-defined columnar map of orientation preference in tree shrew V1, do these changes in the tuning of individual neurons result in detectible changes in the structure of the orientation preference map? By definition, if the orientation preferences of individual neurons change, then the pattern of activity that defines the columnar map has changed because neurons with similar orientation preference are clustered together. But it is important to emphasize the magnitude of the change in orientation preference relative to the tuning width of layer 2/3 neurons and the percentage of neurons that exhibit a change in preference. The median change in preferred orientation for neurons in the S+ flanking region was only 2.35 degrees in the direction of the S+ orientation (see Figure 4E), small relative to the median tuning width of layer 2/3 neurons (55 degrees). In addition, only 16.7% of the neurons in the S+ flank exhibit a significant shift in orientation preference. Because orientation preference maps are based on the average response of populations of neurons to grating stimuli, and the majority of the neurons are unchanged, these changes have no detectible impact on overall map structure. These results emphasize the flexibility of cortical networks to undergo changes in response properties that enhance discrimination without fundamentally altering the overall modular structure of the networks.

Learning-related changes in population discrimination predict additional behavioral performance impacts

In addition to characterizing the single cell tuning properties that contribute to changes in d'_{sc}, the ability to present a broad range of orientations in the passive context allowed us to probe the orientation specificity of the learning-induced changes in neural population discriminability. We computed d'_{pop} between the S+ and orientations within +/− 25 degrees of the S+ in 2.5 degree increments (Figure 5A). Positive offsets from the S+ indicate orientations in the direction of the trained S−, while negative offsets indicate symmetric, untrained orientations. Consistent with task-specificity for learning-related changes, significant improvements ($p<0.05$, Students t-test) in the average (bold trace) population d' for five tree shrews (light traces) reach a peak at 22.5 degrees offset, which is the orientation of the S− (Figure 5A). Interestingly, enhanced neural population discrimination was observed for untrained orientations that lie between the S+ and S− stimuli (e.g. +12.5 degrees) but not for stimuli with orientations displaced away from the S+ (e.g. −12.5 degrees). Indeed, our analysis reveals a weak but significant decrease ($p<0.05$, Students t-test) in d'_{pop} for orientations displaced 25 degrees in this direction from the S+. Given that learning-induced improvements in single cell d' for S+ and fine S− stimuli were localized to neurons with preferred orientations in this range (i.e., S+ flanking neurons), these results raise the possibility that learning may improve the neural discriminability of the trained orientations with consequences for discrimination of nearby untrained orientations.

If the passive increases in neural discrimination reflect changes in V1 activity that support enhanced behavioral performance, this predicts an asymmetric transfer of discrimination enhancement: tree shrews that have learned 22.5 degree discriminations would show an enhanced ability to discriminate the S+ stimulus from untrained +12.5 degree stimuli

compared to −12.5 degree stimuli. To test this prediction, we introduced a novel task to shrews that had been trained on the original S+/S− discrimination. Following the completion of combined imaging and behavioral experiments, tree shrews continued to train in their home cages for at least 10 days in the original task. We then modified the task to include S− stimuli at symmetric offsets from the S+ stimulus at +/− 12.5, 22.5 and 45 degrees. Figure 5B shows the average performance of one shrew on the symmetric Go/No Go task over an initial 10-day period. Consistent with the prediction, there was a conspicuous asymmetry in discrimination performance, with a much lower percentage of Go responses (i.e. correct rejections) for S− stimuli offset by +12.5 degrees from the S+ stimulus (in the direction of the original S− stimulus) than were found for stimuli offset by −12.5 degrees from the S+ stimulus (in the direction away from the original S−). Significant differences in go rates at +12.5 and −12.5 degrees were observed in 4 out of 5 shrews (Figure 5C, left), and as a group median go rate differences were significantly different from zero (Figure 5C, right; $p<0.05$ Student's t-test).

While this asymmetry is consistent with a neural enhancement in discrimination performance for untrained stimuli offset by +12.5 degrees from the S+, we recognized that additional factors may contribute to the high percentage of incorrect responses to untrained stimuli offset by −12.5 from the S+. Indeed, our results show that the neurons best able to discriminate the S+ from the original S− stimuli—the S+ flanking neurons—are especially poor at discriminating the S+ stimulus from nearby stimuli offset in this negative direction (Figure 5D,E). Thus, if the animals have learned to rely on the activity of S+ flanking neurons to signal the presence of the S+ stimulus (i.e., the reward), and these neurons respond in a similar fashion to the S+ stimulus and these neighboring stimuli, poor discrimination performance for these stimuli would be expected. Indeed, not only did animals exhibit an initial asymmetry in discrimination performance, the high Go-rate for negative offset stimuli continued even after 30 days of training, well beyond the normal range of time to reach criterion performance for the original S+/S− stimuli (approximately 1 week; Figure 5F). The magnitude of each shrew's asymmetric Go bias (an approximation of the shrew's internal representation of the S+) was estimated by measuring the offset of the peak of a Gaussian fit of each day's psychometric curve (Figure 5F, top). While there was progressive improvement over time in the Go rate (false alarm rate) for negative offset stimuli at 45 and 22.5 degrees from the S+ stimulus, these improvements reached a plateau for the 12.5 degree offset stimulus (Figure 5F, bottom) - the stimulus predicted to be the least discriminable from the S+ stimulus since it drives a neural population response that has the highest degree of overlap with the population that signifies the presence of the S+.

Together, these results suggest that while Go/No Go training is accompanied by changes in V1 responses that optimize discrimination of the rewarded and distractor stimuli, these changes could be responsible for an orientation specific impairment in discrimination learning of nearby orientations that persists over several weeks. Thus, persistent learning-induced changes in the responses of V1 neurons that are optimized for performance of one behavioral task, may be counter-productive for learning to discriminate other similar visual stimuli.

Discussion

Learning a fine orientation discrimination task is accompanied by persistent changes in the responses of neurons in layer 2/3 of tree shrew V1 that enhance the neural discriminability of task-relevant orientations. This enhancement arises in a select subset of neurons whose preferred orientation is offset from the target stimulus and which, prior to training, endows them with a relatively heightened capacity to discriminate the rewarded and non-rewarded stimuli. With learning, the responses of these neurons to the rewarded stimulus increase, further enhancing the neural discriminability of rewarded and non-rewarded stimuli and doing so in a fashion that selectively augments the population response to the rewarded stimulus. The persistence of these changes outside of the task in which it originated, and the enhancement and impairment of learning in additional discrimination tasks that are predicted by these changes, provide converging lines of evidence that plastic changes in the neural representation of stimulus features by V1 neurons contribute to fine discrimination learning.

The demonstration that neurons in tree shrew V1 can exhibit changes in response to task-relevant stimuli is consistent with previous studies that have shown changes in the response properties of V1 neurons that correlate with behavioral and neural coding performance[3, 4, 6, 9, 37–39]. Many of these studies in the rodent have emphasized that it is the increased response of V1 neurons to the rewarded stimulus (and in some cases the non-rewarded stimulus) that correlates with improved task performance. We also find that increased responses to the rewarded stimulus is the prevailing feature of the learning induced change (found in 66% of altered S+ flanking neurons), followed by a reduction in response to the distractor stimulus (found in 51% of altered S− flanking neurons). Additionally, our results show that learning is accompanied by a dramatic increase in the ability of V1 neurons to discriminate target and distractor stimuli due to a bias in the enhancement of S+ responses to a subset of neurons, S+ flanking neurons, whose tuning at the onset of training is well suited for discriminating the task stimuli. The idea that training selectively enhances the responses of V1 neurons whose tuning profiles make them optimal for discrimination of task stimuli has been suggested before in an orientation discrimination study in primates[11], but subsequent work did not find any changes in the orientation tuning of V1 or V2 cells in a similar paradigm[13]. However, both research groups reported learning-related orientation tuning changes in V4[12, 14]. By tracking the responses of individual neurons over the course of learning, our data supports that idea that a subset of neurons in V1 within a highly organized functional architecture undergoes orientation-specific changes during perceptual learning that are constrained by the information coding properties of neurons relative to the task. However, it remains highly likely that V1 is one of many cortical regions that are relevant for perceptual learning.

Preexisting discrimination capability for task-relevant stimuli cannot be the only factor determining which neurons undergo learning-induced response enhancement. If so, we would expect to see comparable enhancement of the responses of neurons with preferences in the S− stimulus flank to the presentation of the S− stimulus. In fact, while S− and S+ flanking neurons exhibit comparable discrimination of S+ and S− stimuli at the start of training, post-learning, the responses of S− flanking neurons actually exhibit reduced discrimination of the task stimuli, in part due to a reduction in response to the S− stimulus.

Thus, learning in this task appears to selectively enhance the response of neurons with tuning properties that can optimally discriminate the task stimuli and respond preferentially to the rewarded stimulus. In short, learning amplifies the responses of neurons that predict the presence of the rewarded stimulus.

But there are other explanations for this selective enhancement in response that deserve consideration. Previous experiments have shown that repetitive stimulation under passive conditions can give rise to stimulus-specific response potentiation (SRP)[40], raising the question as to whether the increase in the response of S+ flanking neurons could be explained by stimulus repetition rather than reward-association. We believe SRP is an unlikely explanation for our observations since the parameters of stimulus presentation in our experiments are quite different from those that have been associated with SRP. It is true that the S+ stimulus was presented almost twice as frequently as the S− during the course of active participation in the fine discrimination learning paradigm (the total number of S+ and S− presentations was on average 551.2 and 292 presentations, respectively, per animal). However, both of these numbers are small in comparison to the average number of passive stimulus presentations each animal received (8784) and which covered the full range of orientation space. In this context, the S+ stimulus only accounts for approximately 7% of the stimulus presentations. Moreover, the conditions for SRP involve the continuous presentation of a single oriented stimulus for hundreds of seconds. In contrast, in our behavioral experiments, both S+ and S− stimuli are presented, each for a duration of only 0.5 seconds, with multiple seconds to minutes passing between stimulus presentations, and less than 50 presentations per session. Beyond the differences in stimulation parameters, the effects on response properties are also distinctly different. The increase in response is not centered on the neurons that prefer the S+ (as would be expected with SRP), but is shifted to the population best able to discriminate S+ vs S−. Moreover, the visual discrimination learning paradigm employed here results in both increases in response to the S+ stimulus, and a modest reduction in response to the S− stimulus that would not be expected from the unrewarded repetition paradigm. We note that previous studies have observed a stimulus-specific reduction in response under passive viewing conditions when stimuli are behaviorally irrelevant and the reduction we observed could be a similar phenomenon[9, 41]. However, the S− stimulus in our paradigm is not completely irrelevant to the behavior, providing useful information for the animal's decision to lick or not.

It is also important to emphasize that the learning induced changes in response described here are likely to reflect the specific features of the behavioral task. The task employed here requires discrimination of orientations that activate overlapping distributions of neurons, and the neurons that are optimal for predicting the presence of the rewarded stimulus are those that have orientation preferences in the S+ flanks. For performance of Go/No Go tasks that do not require fine discrimination (e.g. 90 degree offset), reliable prediction of the rewarded stimulus could be achieved by response enhancement of neurons that prefer the rewarded stimulus, consistent with results in rodents[4, 9 37]. Also, the Go/NoGo task employed here is structured so that only one of the stimuli is associated with reward, and enhancement of a single population of neurons achieves both reliable discrimination and identification of the rewarded stimulus. If instead the task was structured so that both stimuli were associated with reward, and discrimination was necessary to determine the appropriate

action required to achieve reward (e.g.,2-alternative forced choice, A/B, or same/different tasks) the changes might involve enhancement of two populations of neurons with preferred orientations arranged symmetrically around both stimulus flanks. It remains to be seen just how flexibly the circuits in V1 can be altered to enable different types of discriminations under different task conditions.

Our results demonstrate that the selective enhancement of the responses of V1 neurons is not confined to the behavioral paradigm, but is maintained under passive viewing conditions. Such persistence would be expected if the changes in V1 contribute to the improvement in task performance that persists across days and weeks. This also indicates that these changes reflect fundamental alterations in the representation of visual stimuli by V1 neurons, rather than context-dependent neuromodulatory effects, which are known to regulate neural responses in V1[42–44]. Of course, this does not rule out the contribution of context-dependent modulatory effects to task performance. Indeed, enhancement effects under the passive presentation conditions are weaker than those observed during task participation, suggesting that the persistent changes in V1 responses combine with modulatory effects to enable highly reliable behavioral performance.

Further evidence for persistence of the changes in V1 responses beyond the behavioral paradigm in which they emerged came from additional experiments where animals were required to discriminate the S+ stimulus from nearby orientations with either a positive offset (towards the S−) or a negative offset (away from the S−). Although perceptual learning effects are generally regarded as being highly selective for the learned stimuli[4, 8, 9, 45], the persistent learning induced changes in neural population response that we found predicted impacts on these novel discriminations—both enhancement and impairment—that were evident in the animals' behavioral performance. The enhancement in the acquisition of discriminations for positive offset orientations is consistent with the persistent enhancement in the discrimination capability of S+ flanking neurons and the fact that analysis shows that this extends to the novel positive offset stimulus orientation. Thus, the activity of the S+ flanking neurons continues to be highly predictive of reward, responding strongly to the S+ stimulus and weakly to both the S− and the novel nearby orientation.

The impairment in the discrimination of the S+ stimulus from nearby stimuli with negative offsets is also predictable from the persistent enhancement in the response of S+ flanking neurons to the S+ stimulus since the enhancement reduces the difference in the pattern of population activity evoked by the S+ stimulus and these nearby orientations. This result is reminiscent of the classical psychophysical phenomenon known as the peak shift effect, in which the learning of S+/S− discriminations of a broad range of multisensory features leads to a heightened response rate for untrained stimuli neighboring the S+[46, 47]. In psychological terms, this effect is considered a form of generalization learning, in which trained stimulus attributes are generalized across a range of untrained stimulus features. Our results suggest that what has been described as a generalization of the S+ stimulus to neighboring orientations is, in fact, a byproduct of a learned, neural specialization for discrimination of the original S+ and S−, which results in impairment of discriminations between the S+ and nearby orientations with negative offset.

But what accounts for the persistent impairment in the animals' ability to learn to discriminate the S+ stimulus from these nearby orientations in spite of extensive training? Given that changes in neuronal response that were associated with learning of the initial task reduced the neural discrimination of the S+ and these nearby orientations, additional changes in neuronal response are likely to be necessary to achieve reliable behavioral discrimination of these stimuli. These changes would include a reduction in the response of the S+ flanking neurons to the S+ stimulus, and an increase in response to the S+ stimulus by neurons with preferences biased towards the original S− stimulus. Both of these changes would have the effect of reducing the neural discriminability of the S+ stimulus from the S− and negative offset stimuli, and reduce the overall reliability of the V1 signal in predicting the presence of the rewarded stimulus in the task. This is because the persistent changes from learning the original task should enable the activity of the S+ flanking neurons to continue to be a good over-all predictor of reward in the second task, discriminating the S+ stimulus from the S− and negative offset stimuli, even without accurate discrimination of the positive offset stimulus. These considerations emphasize that changes in the responses of V1 neurons required to achieve fine discrimination learning demonstrated here have constraints that are ultimately defined by the orientation tuning selectivity of individual neurons and by the training context in which the stimuli are presented. Thus, circuit level changes that enable enhanced population coding necessary for one discrimination can be detrimental to others, akin to a zero-sum game at the level of behavior. At the neural coding level, this resembles an economical process involving gains in discrimination while minimizing, but not eliminating losses in performance.

While neurons in V1 exhibit learning-related response changes, the locus of the events responsible for these changes and the underlying synaptic mechanisms remain unclear. The orientation selectivity of the effects provides some constraint on the locus: at or beyond the emergence of orientation selective responses along the visual pathway. In the tree shrew, orientation selective responses emerge first in cortical layer 2/3[48], so it is possible that the effects result from local synaptic changes within V1 layer 2/3 circuits, mediated by the impact of reward-related neuromodulatory inputs[42, 49, 50]. However, given that orientation selectivity is a property shared by neurons throughout extrastriate cortex, modulated patterns of activity from a wide range of top-down and/or reciprocally connected cortical areas[51–53], could be critical for these changes. Uncertainty about the locus of the changes is made even more challenging by the diversity of changes in the tuned responses of V1 neurons to the S+ and S− stimulus revealed by our chronic analysis of single cell behavior. That diversity, combined with the fact that the majority of the neurons in our sample exhibited no significant change in response during the course of learning, suggests that the plasticity mechanisms responsible for learning engage cortical networks with a degree of specificity that extends beyond the orientation preferences relevant for the task discrimination. Further studies exploring the identity of the neurons that undergo learning induced change, their patterns of connections, and the synaptic bases for the changes are necessary to fully understand how changes in V1 responses contribute to training enhanced perceptual discrimination.

STAR Methods

RESOURCE AVAILABILITY

Lead Contact and Materials Availability—Further information and requests for resources and reagents should be directed and will be fulfilled by the lead contact, David Fitzpatrick (david.fitzpatrick@mpfi.org). This study did not generate new unique reagents.

Data and Code Availability

- Due to the large size and number of files associated with the imaging dataset, the full dataset has not been uploaded to a public repository. A subset of the data is available from Harvard Dataverse (https://doi.org/10.7910/DVN/O1CHOV). All data reported in this paper will be shared by the lead contact upon request.
- Code used for data collection, data processing, and analysis are available via Github (https://github.com/joschumacher/Schumacher_et_al_SelectiveEnhancementV1).
- Any additional information required to reanalyze the data reported in this paper is available from the lead author upon request.

EXPERIMENTAL MODEL AND SUBJECT DETAILS

All experimental procedures were performed in accordance with NIH guidelines and were approved by the Max Planck Florida Institute for Neuroscience Institutional Animal Care and Use Committee. Tree shrew (*Tupaia belangeri*, n = 16, approximately 6 – 36 months of age, male and female) numbers were minimized to conform to ethical guidelines. Of the animals included in this study, 5 were included in combined imaging and behavioral experiments, two were included in electrophysiological verification of optogenetics, two were included in the optogenetic perturbation of behavior, and 7 provided additional behavioral data.

METHOD DETAIL

Surgery and Viral Expression—Tree shrews were first anesthetized with Midazolam (5 mg/kg, IM), Ketamine (75 mg/kg, IM). Atropine (0.5 mg/kg, SC) was administered to reduce secretions, Dexamethasone (1 mg/kg, IM) was given to reduce inflammation during surgery, and Buprenorphine SR provided a long lasting analgesic for post-operative recovery. The animal's head was shaved, and any remaining hair was removed with Nair. The surgical site was injected with a mixure of bupivacaine and lidocaine (0.3 – 0.5 ml, SC). A mixture of oxygen, nitrous oxide (O2/N20 1:0 to 1:2) and gas anesthesia (isoflurane 0.5 to 2%) were initially delivered through a mask and later switch to an intubation tube. Venous cannulation (tail or hind limb) and tracheal intubation were established after the animal no longer responded to a toe-pinch. Internal temperature was maintained by thermostatically controlling a heating pad. Expired CO_2 and heart rate were monitored for any signs of stress. The respiration rate (100 to 120 strokes per minute) was regulated through a ventilator. The animal was placed in a stereotaxic device (Kopf, Model 900 Small Animal Stereotaxic Instrument). A small incision was made in the scalp, and skin and muscle were retracted. After cleaning the underlying skull, the metal headpost and cranial imaging

chamber (centered over V1) were affixed to the skull with metabond (C & B), and dental acrylic (Ortho-Jet, Lang). The skin and muscle were then unretracted, cut to overlap with the edge of the dental acrylic, and secured in place with vetbond. A circular craniotomy (approx. 6mm diameter) was performed in the center of the cranial imaging chamber with a small drill to expose the dura. In some cases the headpost was implanted separately from the imaging chamber, but the imaging chamber was always implanted along with viral injections.

Visual cortex was injected with a virus expressing GCaMP6s (*AAV9.Syn.GCaMP6s.WPRE.SV40,* Penn Vector Core/Addgene, a gift from Douglas Kim and GENIE Project[30]; *AAV1.hSyn1.mRuby2.GSG.P2A.GCaMP6s.WPRE.SV40,* Addgene, a gift from Tobias Bonhoeffer & Mark Huebener & Tobias Rose[56]) at 3 to 5 sites (1–2 μl; 1E13 GC/ml) through a beveled glass micropipette (15 to 25 μm tip diameter, Drummond Scientific) using a pressure injector (Drummond Nanoject II), at 200 and 400 μm from the cortical surface. After a brief waiting period, a durotomy was performed within the craniotomy, and a double-layered cover slip composed of a small round glass coverslip (3 – 5mm diameter, 0.7mm thickness, Warner Instruments) glued to a larger coverslip (8mm diameter, 0.17 mm thickness, Electron Microscopy Sciences) with an optical adhesive (Norland Optical Adhesive 71) was placed into the chamber with the thick coverglass gently resting on the brain). The top layer of coverglass was held in place with a snap ring (5/16” internal retaining ring, McMaster-Carr) and sealed with a layer of Vetbond. After sealing the imaging chamber, Neosporin was applied to the wound margin and animals recovered from anesthesia on a heating blanket. Post-operative care included antibiotics (Baytril, 5 mg/kg), and following the timecourse of Buprenorphine SR, anti-inflamatories (Metacam, 0.5mg/kg).

Two-photon calcium imaging and data processing—Imaging experiments were performed using a Bergamo II Series Microscope (Thorlabs) using 920 nm excitation provided by a Mai Tai DeepSee laser (Spectra-Physics) running Scanimage 2015 or 2018 (Vidrio Technologies) and an FPGA module (PXIe-6341, FlexRIO, National Instruments). Average excitation power at the objective (16x, CF175, Nikon Insttuments) ranged from 40 to 100 mW. Images were acquired at 15 Hz (512×512 pixel field of view ranging from 1.19 to 1.85 μ/pixel) Two-photon frame triggers from Scanimage and events denoting visual stimuli and phases of behavioral trials were recorded using Spike2 (CED, Cambridge, UK).

In 5 tree shrews, imaging was carried out across training sessions. Prior to data acquisition, the imaging site was located by matching the FOV to known anatomical features from prior recordings, such as blood vessel patterns and somata locations.

Aberrant neural responses properties of an unknown origin led to the exclusion of one additional animal from this study. Population responses recorded during behavioral performance did not appear to be stimulus specific, and therefore formed no basis for neural discrimination. Inclusion of this animal in our analyses essentially added noise to our measurements and did not alter our results, but the data are excluded nonetheless on the basis of their known abnormality.

Intrinsic Signal Imaging—Intrinsic signal imaging was performed using a custom setup including a Xyla sCMOS camera (Andor) controlled by μManager2 software. Intrinsic hemodynamic responses were obtained by illuminating the surface of the brain with a 630nm red LED (Thorlabs). Maps of azimuth and elevation were generated by stimulating visually evoked responses with a vertical or horizontal black bar placed at a range of offsets from the center of gaze (azimuth: 0 to 30 degrees in 3 degree increments; elevation: −20 to +20 degrees in 4 degree increments). The position of the bar was jittered within +/− 0.5 degrees during the 4 second stimulation.

Visual stimulation—Visual stimuli were displayed on a LED monitor with a resolution of 1920 × 1080 pixels and refresh rate of 120 Hz, which was centered in front of the animal at a distance of 25 cm from the eyes. Stimuli were generated using Psychopy2 written in Python.

Behavioral training—Behaviorally-trained animals had a normal diet consisting of food pellets and supplemental fruits, vegetables, and mealworms. Trained tree shrews were water restricted, but received a minimum of 60 ml/kg of water per training day through a combination of earned rewards and daily allotments. At least twice weekly on non-training days, the shrews received at least 150ml/kg of water. All water restricted shrews were monitored daily for maintenance of body condition. Tree shrews were shaped and trained to perform a coarse visual discrimination task (>=45 degrees) over the course of one to two weeks before learning to perform a fine discrimination task (22.5 degrees). Initial shaping and familiarity with the apparatus was achieved in freely moving animals in a behavioral annex that was either attached to their home cage or attached to the imaging table. The annexes were 13” long × 6” tall × 8” wide, and comprised of a wire mesh with an adhesive plastic coating, an anodized metal floor plate, and a plexiglass screen for viewing the stimulus monitor. The reward/response port passed through the plexiglass screen, at a distance that preserved the spatial frequency of oriented grating.

The animals were gradually acclimated to handling, weighing, transportation between the animal facility and imaging, and learning to lick a response port for liquid reward over the course of weeks. Liquid rewards were RO water or a 1:1 dilution of apple juice in RO water depending on animal preference. Reward delivery was controlled by a syringe pump with custom electronics (custom parts or BS-8000, Braintree Scientific) through a gavage needle that acted as a capacitive sensor for lick detection through a custom Arduino Uno interface. Animals that showed a willingness to acquire liquid rewards in the absence of a task in the imaging room were acclimated to head fixation and tube restraint over several days in increasingly long durations starting with under a minute and lasting up to 30 minutes. Animals that showed a willingness to acquire liquid rewards while head-fixed were candidates for visual discrimination learning and imaging. Some animals that were not used in head-fixed experiments were able to perform in the freely-behaving setup, and are included in the characterization of behavioral performance (Fig. 1).

During behavioral training, a trial started when the tree shrew licked the reward port. Following a variable delay period (2.5 to 3.5 seconds), the S+ or S− was presented for 0.5 seconds (90–100% contrast, static square wave grating). To match V1 sensitivity, the spatial frequency of the gratings was 0.25 cycles per degree[48]. To ensure that orientation

was the only feature distinguishing the S+ and S−, grating phase was randomized. Following presentations of the S+, licking in the 1 second response period elicited a liquid reward (hit trial), and failing to lick resulted in a time out (miss trial). Following presentations of the S−, licking in the response period elicited a time out (false alarm, FA), while withholding a response (correct rejection, CR) queued up a subsequent S+ presentation and response period. These guaranteed S+ stimuli were not factored into the quantification of the animal's behavioral performance, but rather incentivized CRs. Behavioral performance was measured using behavioral d-prime,

$$d' = \Phi^{-1}(\text{Hit Rate}) - \Phi^{-1}(\text{FA Rate}),$$

where Φ^{-1} is the normal inverse cumulative distribution function[4]. Early on in training, the timing of responses was shaped by delivering a small bolus of liquid reward on a subset of trials (hints). As response timing improved, the probability of hinted trials was decreased gradually to zero across sessions.

Experimental timeline—Tree shrews were imaged across training sessions of fine discrimination. Training sessions lasted approximately 1 hour, and were immediately followed by passive stimulus presentations. After reaching criterion performance and completing their imaging sessions, shrews maintained their behavioral performance by performing the task freely moving in a behavioral annex attached to their homecage. Subsequent behavioral testing of untrained S− orientations was conducted after approximately 10 days of baseline annex training of the original task.

Electrophysiology—To evaluate the efficacy of optogenetic interneuron stimulation, whole-cell patch clamp and juxtasomal recordings in two anesthetized tree shrews expressing ChR2 under control of the mDlx enhancer. The virus (AAV2/1.mDlx.ChR2-FLAG-Kv2.1.p2a.H2b-CyRFP) was generated as a custom preparation from Vigene for Wilson et al. (2018)[29], based on a ChR2 construct provided by by Baker et al. (2016)[57]. Recordings were performed by inserting a pipette through an agarose-filled craniotomy covered with a coverglass with a small hole drilled for pipette access. These procedures have been described elsewhere[29] but briefly, a silver-silver chloride reference wire was inserted below the muscle. Recordings were made in current clamp mode using custom Labview software. Pipettes of 5 – 9 MOhm resistence were pulled using borosilicate glass (King Precision Glass) and filed with an intracellular solution containing (in mM) 135 K gluconate, 4 KCl, 10 HEPES, 10 Na_2-phosphocreatine, 4 Mg-ATP, 0.3 Na_3GTP, pH 7.2, 295 mOsm. Neurons were recorded from layer 2/3 (100 to 300 um below the cortical surface). Using a Multiclamp 700b (Molecular Devices). Series resistance and pipette capacitance were corrected online, and analog signals were digitized using Spike2 (CED). For optogenetic inactivation, a fibre (1mm, NA 0.63) coupled to a 455 nm LED light source (Prizmatix) was lowered to 3mm above the cover glass. Light power at the cortical surface varied from 1 to 16 mW/mm^2. Optogenetic stimulation coinciding with visual stimulation started with a brief ramp (100ms) before visual stimulation.

Recordings took place after two weeks of viral expression. Viral injections for acute procedures in tree shrews are similar to those for chronic procedures described above and have been described previously[48], but don't involve implantation of a head-post or chamber, and require only small burr holes rather than a full craniotomy. For electrophysiological recordings, tree shrews were first anesthetized with Midazolam (100 mg/kg, IM) and Ketamine (100 mg/kg, IM) and atropine (0.5 mg/kg, SC) was administered to reduce secretions. A peripheral venous cannula was inserted in the hind limb to allow fluids delivery (10% dextrose in LRS) during surgery. The incision site was treated with a mixture of lidocaine and bupivacaine (0.3 – 0.5 ml, SC) and ear bars were coated with lidocaine ointment (5%). Gas anesthesia was administered as described above in the surgical procedures, and maintained throughout the duration of the craniotomy procedure and experiment. The recording chamber was identical to our typical imaging chamber described above, with the addition of metal extension for head fixation.

Optogenetic inhibition of bilateral V1 activity—One male and one female adult tree shrew were used for combined visual discrimination behavior and optogenetic stimulation of channelrhodopsin under the control of the mDlx enhancer (pAAV-mDlx-ChR2-mCherry-Fishell-3 was a gift from Gordon Fishell[28], Addgene plasmid # 83898, packaged into AAV9 by Vigene). The shrews were first trained to perform the visual discrimination task to proficiency (d' > 1). Headpost, window implantation and viral expression procedures were the same as described for GCaMP6s experiments with slight modifications to allow for bilateral windows. Rather than implanting a metal chamber 5mm diameter circular craniotomies were made over bilateral V1 using a 5mm disposable biopsy punch (Integra Miltex). A window comprised of one 4.5mm coverglass (0.7mm thick) was affixed to a wider 8mm coverglass (0.17mm thick) with optical adhesive, and following a full durotomy the thick coverglass was placed in the craniotomy on the surface of the brain. The coverglass was sealed in place with vetbond and dental acrylic.

After recovery from surgery, tree shrews resumed behavioral practice with interleaved trials of light stimulation that ramped up and down 100 ms before and after stimulus onset.. Optical fibers were inserted into 3d printed black plastic cylinders that were fit to the surface of the cranial windows to provide sealed light stimulation, support the optical fiber at a fixed distance from the surface of the glass, and ensure uniform illumination. Light intensity was calibrated using both thermal and photodiode light power sensors (Thorlabs), and ranged from 0 to 8 mW/mm^2.

QUANTIFICATION AND STATISTICAL ANALYSIS

Imaging data were first corrected for motion and drift using customized image registration software written in Matlab (Mathworks). Cellular regions of interest (ROIs) corresponding to visually identified neurons were assigned using ImageJ by either inspecting frames of an imaging stack, or the average intensity or standard deviation z-projections of the imaging stack. The fluorescence time series of each cell was measured by averaging all pixels within the ROI over time. Evoked fluorescence signals were calculated as $dF/F=(F–F_0)/F_0$, where F_0 is the baseline fluorescence signal averaged over 0.5 seconds before stimulus onset, and F is the average fluorescence signal during the stimulus presentation.

Orientation tuning curves were measured by calculating the mean dF/F for each orientation. Preferred orientation was calculated by computing a vector sum of the tuning curve and measuring angle of the resultant vector in polar coordinates (CircStat Toolbox[58]). Tuning curve bandwidth was calculated by first least-squares fitting a double Gaussian to the tuning curve, and taken as the full width at half max of the Gaussian function to the nearest degree. Single neurons were defined as orientation tuned based values of 1 – circular variance (CV) > 0.25 which was defined as

$$\left|\frac{\sum_k R(\theta_k)\exp(2i\theta_k)}{\sum_k R(\theta_k)}\right|$$

Where θ_k is the orientation of a visual stimulus and R(θ_k) is the response to that stimulus. Statistical significance of shifts in orientation preference were measured with a Watson-Williams two sample test for equal means in circular data (CircStat Toolbox[58]). Statistical significance of changes in S+, S−, or preferred orientation response magnitude were calculated using Wilcoxon rank sum tests between pre- and post- response distributions. We quantified changes in the underlying shape of the neuronal orientation tuning curve by measuring an Asymmetry Index before and after learning. First, the orientation tuning curve was fit with a spline. The spline-fit curve was then aligned with it's peak response at the center, and the area under the curve of the left and right halves of the tuning curve were computer. The asymmetry index is defined as

$$\frac{A_1 - A_2}{A_1 + A_2},$$

where $A1$ is the area under the right side of the curve and A2 is the area under the left side of the curve. For reference, an S+ flanking neuron would have A_1 facing the S+ and A_2 away from the S+, while an S− flanking neuron would have A_2 facing the S− and A_1 away from the S−.

We quantified the neural discriminability of pairs of behaviorally relevant stimuli at the neural population level using a population d' neurometric (d'$_{pop.}$). This metric takes dimensionality reduction approach to mitigate the complexity of the simultaneous responses of many cells to a lower dimensional space in which separability analyses can be performed. First, the population response on each trial is organized as an nx1 dimensional vector of ΔF/F, where n is the number of cells in the neural population. We then computed the mean population response to each stimulus, and projected each high dimensional single trial response onto the vector between the two mean responses. Neural discriminability between pairs of stimuli is then quantified as the d' of distributions of single trial responses in this 1d space,

$$d'_{pop.} = \frac{\mu_1 - \mu_2}{\left(\frac{1}{2}\left(\sigma_1^2 + \sigma_2^2\right)\right)^{\frac{1}{2}}},$$

where μ_1 and μ_2 were the mean position in the 1d space, and $\sigma_{1 \text{ and }} \sigma_2$ were the standard deviations of those posltions.

Using passively recorded responses, we also analyzed $d'_{pop.}$between the S+ and other orientations spanning +/− 45 degrees around the S+ (Fig. 5a). Here, the 1d discrimination space was determined by the vector between mean responses to the S+ orientation and either positive or negative 25 degrees from the S+, depending on the offset of the paired orientation from the S+.

We quantified the neural discriminability of pairs of behaviorally relevant stimuli at the single neuron level using a single cell d' neurometric (d'_{sc}),

$$d'_{sc} = \frac{\mu_1 - \mu_2}{\left(\frac{1}{2}\left(\sigma_1^2 + \sigma_2^2\right)\right)^{\frac{1}{2}}},$$

where μ_1 and μ_2 were the mean responses of two different stimuli, and $\sigma_{1 \text{ and }} \sigma_2$ were the standard deviations of responses to those stimuli.

Population responses (Fig. 3c, Fig. 5d,e), and d'_{sc} profiles (Fig. 3d, Fig. 5d,e) were computed using a moving window (mean +/− SEM) of ΔF values within 10 degree bins in 5 degree increments. $\Delta d'_{sc}$ profiles were computed using the same procedure with 20 degree bins to increase the number of cells per bin for statistical testing.

To measure the persistence of behavioral bias of each shrew toward novel S− stimuli in the second set of behavioral experiments (Fig. 5f), we least-squares fit each day's psychometric function (e.g. Fig. 2b, top) with a Gaussian. The shrew's approximated S+ (the S+ inferred from the shrew's behavioral performance) was taken as the peak orientation of this Gaussian function (e.g. Fig. 5f, top).

Statistics—For paired comparisons across conditions or sessions we used the Wilcoxon signed-rank test or a paired t-test. For unpaired hypothesis testing of significant differences in response parameters from zero, we used the Wilcoxon signed-rank test or Student's t-test. We report Pearson's correlation coefficient for all correlations. N's and p-values are reported in the text and figure legends.

Supplementary Material

Refer to Web version on PubMed Central for supplementary material.

Acknowledgements:

We thank Theo Walker, Val Hoke, and Susan Freling for their assistance with behavioral training and tree shrew care, Dan Wilson and Ben Scholl for expertise with electrophysiological recordings, and Amanda Jacob, Rachel Satterfield, and Nicole Shultz for tissue processing and lab support. We also thank members of the Fitzpatrick lab and the MPFI community, especially Gabriela Rodriguez for support and helpful comments throughout this project. This work was supported by and F32 EY028430 (J.W.S.), R01 EY006821 (D.F.), and Max Planck Florida Institute for Neuroscience.

References

1. Hubel DH, and Wiesel TN (1959). Receptive fields of single neurones in the cat's striate cortex. The Journal of physiology 148, 574–591. [PubMed: 14403679]
2. Marshel JH, Kim YS, Machado TA, Quirin S, Benson B, Kadmon J, Raja C, Chibukhchyan A, Ramakrishnan C, Inoue M, et al. (2019). Cortical layer-specific critical dynamics triggering perception. Science 365.
3. Jurjut O, Georgieva P, Busse L, and Katzner S (2017). Learning Enhances Sensory Processing in Mouse V1 before Improving Behavior. The Journal of neuroscience : the official journal of the Society for Neuroscience 37, 6460–6474. [PubMed: 28559381]
4. Poort J, Khan AG, Pachitariu M, Nemri A, Orsolic I, Krupic J, Bauza M, Sahani M, Keller GB, Mrsic-Flogel TD, et al. (2015). Learning Enhances Sensory and Multiple Non-sensory Representations in Primary Visual Cortex. Neuron 86, 1478–1490. [PubMed: 26051421]
5. Danka Mohammed CP, and Khalil R (2020). Postnatal Development of Visual Cortical Function in the Mammalian Brain. Frontiers in systems neuroscience 14, 29. [PubMed: 32581733]
6. Gilbert CD, and Li W (2012). Adult visual cortical plasticity. Neuron 75, 250–264. [PubMed: 22841310]
7. Carandini M, and Churchland AK (2013). Probing perceptual decisions in rodents. Nature neuroscience 16, 824–831. [PubMed: 23799475]
8. Goltstein PM, Coffey EB, Roelfsema PR, and Pennartz CM (2013). In vivo two-photon Ca2+ imaging reveals selective reward effects on stimulus-specific assemblies in mouse visual cortex. The Journal of neuroscience : the official journal of the Society for Neuroscience 33, 11540–11555. [PubMed: 23843524]
9. Henschke JU, Dylda E, Katsanevaki D, Dupuy N, Currie SP, Amvrosiadis T, Pakan JMP, and Rochefort NL (2020). Reward Association Enhances Stimulus-Specific Representations in Primary Visual Cortex. Current biology : CB 30, 1866–1880 e1865. [PubMed: 32243857]
10. Hua T, Bao P, Huang CB, Wang Z, Xu J, Zhou Y, and Lu ZL (2010). Perceptual learning improves contrast sensitivity of V1 neurons in cats. Current biology : CB 20, 887–894. [PubMed: 20451388]
11. Schoups A, Vogels R, Qian N, and Orban G (2001). Practising orientation identification improves orientation coding in V1 neurons. Nature 412, 549–553. [PubMed: 11484056]
12. Raiguel S, Vogels R, Mysore SG, and Orban GA (2006). Learning to see the difference specifically alters the most informative V4 neurons. The Journal of neuroscience : the official journal of the Society for Neuroscience 26, 6589–6602. [PubMed: 16775147]
13. Ghose GM, Yang T, and Maunsell JH (2002). Physiological correlates of perceptual learning in monkey V1 and V2. Journal of neurophysiology 87, 1867–1888. [PubMed: 11929908]
14. Yang T, and Maunsell JH (2004). The effect of perceptual learning on neuronal responses in monkey visual area V4. The Journal of neuroscience : the official journal of the Society for Neuroscience 24, 1617–1626. [PubMed: 14973244]
15. Li W, Piech V, and Gilbert CD (2008). Learning to link visual contours. Neuron 57, 442–451. [PubMed: 18255036]
16. Yan Y, Rasch MJ, Chen M, Xiang X, Huang M, Wu S, and Li W (2014). Perceptual training continuously refines neuronal population codes in primary visual cortex. Nature neuroscience 17, 1380–1387. [PubMed: 25195103]
17. Fitzpatrick D (1996). The functional organization of local circuits in visual cortex: insights from the study of tree shrew striate cortex. Cereb Cortex 6, 329–341. [PubMed: 8670661]
18. Bosking WH, Zhang Y, Schofield B, and Fitzpatrick D (1997). Orientation selectivity and the arrangement of horizontal connections in tree shrew striate cortex. The Journal of neuroscience : the official journal of the Society for Neuroscience 17, 2112–2127. [PubMed: 9045738]
19. Bosking WH, Crowley JC, and Fitzpatrick D (2002). Spatial coding of position and orientation in primary visual cortex. Nature neuroscience 5, 874–882. [PubMed: 12195429]
20. Young ME, Sutherland SC, and McCoy AW (2018). Optimal go/no-go ratios to maximize false alarms. Behavior research methods 50, 1020–1029. [PubMed: 28664243]

21. O'Connor DH, Peron SP, Huber D, and Svoboda K (2010). Neural activity in barrel cortex underlying vibrissa-based object localization in mice. Neuron 67, 1048–1061. [PubMed: 20869600]
22. Histed MH, Carvalho LA, and Maunsell JH (2012). Psychophysical measurement of contrast sensitivity in the behaving mouse. Journal of neurophysiology 107, 758–765. [PubMed: 22049334]
23. Andermann ML, Kerlin AM, and Reid RC (2010). Chronic cellular imaging of mouse visual cortex during operant behavior and passive viewing. Frontiers in cellular neuroscience 4, 3. [PubMed: 20407583]
24. Abraham NM, Spors H, Carleton A, Margrie TW, Kuner T, and Schaefer AT (2004). Maintaining accuracy at the expense of speed: stimulus similarity defines odor discrimination time in mice. Neuron 44, 865–876. [PubMed: 15572116]
25. Smear M, Shusterman R, O'Connor R, Bozza T, and Rinberg D (2011). Perception of sniff phase in mouse olfaction. Nature 479, 397–400. [PubMed: 21993623]
26. Snyder M, Hall W, and Diamond I (1966). Vision in tree shrews (Tupia glis) after removal of striate cortex. Psychonomic Science 6, 243–244.
27. Petry HM, and Bickford ME (2019). The Second Visual System of The Tree Shrew. The Journal of comparative neurology 527, 679–693. [PubMed: 29446088]
28. Dimidschstein J, Chen Q, Tremblay R, Rogers SL, Saldi GA, Guo L, Xu Q, Liu R, Lu C, Chu J, et al. (2016). A viral strategy for targeting and manipulating interneurons across vertebrate species. Nature neuroscience 19, 1743–1749. [PubMed: 27798629]
29. Wilson DE, Scholl B, and Fitzpatrick D (2018). Differential tuning of excitation and inhibition shapes direction selectivity in ferret visual cortex. Nature 560, 97–101. [PubMed: 30046106]
30. Chen TW, Wardill TJ, Sun Y, Pulver SR, Renninger SL, Baohan A, Schreiter ER, Kerr RA, Orger MB, Jayaraman V, et al. (2013). Ultrasensitive fluorescent proteins for imaging neuronal activity. Nature 499, 295–300. [PubMed: 23868258]
31. Dadarlat MC, and Stryker MP (2017). Locomotion Enhances Neural Encoding of Visual Stimuli in Mouse V1. The Journal of neuroscience : the official journal of the Society for Neuroscience 37, 3764–3775. [PubMed: 28264980]
32. Cohen MR, and Maunsell JH (2009). Attention improves performance primarily by reducing interneuronal correlations. Nature neuroscience 12, 1594–1600. [PubMed: 19915566]
33. Chisum HJ, Mooser F, and Fitzpatrick D (2003). Emergent properties of layer 2/3 neurons reflect the collinear arrangement of horizontal connections in tree shrew visual cortex. The Journal of neuroscience : the official journal of the Society for Neuroscience 23, 2947–2960. [PubMed: 12684482]
34. O'Keefe LP, Levitt JB, Kiper DC, Shapley RM, and Movshon JA (1998). Functional organization of owl monkey lateral geniculate nucleus and visual cortex. Journal of neurophysiology 80, 594–609. [PubMed: 9705453]
35. Ringach DL, Shapley RM, and Hawken MJ (2002). Orientation selectivity in macaque V1: diversity and laminar dependence. The Journal of neuroscience : the official journal of the Society for Neuroscience 22, 5639–5651. [PubMed: 12097515]
36. Vogels R (1990). Population coding of stimulus orientation by striate cortical cells. Biological cybernetics 64, 25–31. [PubMed: 2285759]
37. Khan AG, Poort J, Chadwick A, Blot A, Sahani M, Mrsic-Flogel TD, and Hofer SB (2018). Distinct learning-induced changes in stimulus selectivity and interactions of GABAergic interneuron classes in visual cortex. Nature neuroscience 21, 851–859. [PubMed: 29786081]
38. Keller AJ, Houlton R, Kampa BM, Lesica NA, Mrsic-Flogel TD, Keller GB, and Helmchen F (2017). Stimulus relevance modulates contrast adaptation in visual cortex. eLife 6.
39. Pakan JM, Francioni V, and Rochefort NL (2018). Action and learning shape the activity of neuronal circuits in the visual cortex. Current opinion in neurobiology 52, 88–97. [PubMed: 29727859]
40. Frenkel MY, Sawtell NB, Diogo AC, Yoon B, Neve RL, and Bear MF (2006). Instructive effect of visual experience in mouse visual cortex. Neuron 51, 339–349. [PubMed: 16880128]

41. Makino H, and Komiyama T (2015). Learning enhances the relative impact of top-down processing in the visual cortex. Nature neuroscience 18, 1116–1122. [PubMed: 26167904]
42. Pinto L, Goard MJ, Estandian D, Xu M, Kwan AC, Lee SH, Harrison TC, Feng G, and Dan Y (2013). Fast modulation of visual perception by basal forebrain cholinergic neurons. Nature neuroscience 16, 1857–1863. [PubMed: 24162654]
43. Pafundo DE, Nicholas MA, Zhang R, and Kuhlman SJ (2016). Top-Down-Mediated Facilitation in the Visual Cortex Is Gated by Subcortical Neuromodulation. The Journal of neuroscience : the official journal of the Society for Neuroscience 36, 2904–2914. [PubMed: 26961946]
44. Lee AM, Hoy JL, Bonci A, Wilbrecht L, Stryker MP, and Niell CM (2014). Identification of a brainstem circuit regulating visual cortical state in parallel with locomotion. Neuron 83, 455–466. [PubMed: 25033185]
45. Jehee JF, Ling S, Swisher JD, van Bergen RS, and Tong F (2012). Perceptual learning selectively refines orientation representations in early visual cortex. The Journal of neuroscience : the official journal of the Society for Neuroscience 32, 16747–16753a. [PubMed: 23175828]
46. Spence KW (1937). The differential response in animals to stimuli varying within a single dimension. Psychological Review 44, 430–444.
47. Hanson HM (1959). Effects of discrimination training on stimulus generalization. Journal of experimental psychology 58, 321–334. [PubMed: 13851902]
48. Lee KS, Huang X, and Fitzpatrick D (2016). Topology of ON and OFF inputs in visual cortex enables an invariant columnar architecture. Nature 533, 90–94. [PubMed: 27120162]
49. Chubykin AA, Roach EB, Bear MF, and Shuler MG (2013). A cholinergic mechanism for reward timing within primary visual cortex. Neuron 77, 723–735. [PubMed: 23439124]
50. Kang JI, Huppe-Gourgues F, and Vaucher E (2014). Boosting visual cortex function and plasticity with acetylcholine to enhance visual perception. Frontiers in systems neuroscience 8, 172. [PubMed: 25278848]
51. Zhang S, Xu M, Kamigaki T, Hoang Do JP, Chang WC, Jenvay S, Miyamichi K, Luo L, and Dan Y (2014). Selective attention. Long-range and local circuits for top-down modulation of visual cortex processing. Science 345, 660–665. [PubMed: 25104383]
52. Pho GN, Goard MJ, Woodson J, Crawford B, and Sur M (2018). Task-dependent representations of stimulus and choice in mouse parietal cortex. Nature communications 9, 2596.
53. Liu D, Deng J, Zhang Z, Zhang ZY, Sun YG, Yang T, and Yao H (2020). Orbitofrontal control of visual cortex gain promotes visual associative learning. Nature communications 11, 2784.
54. Schindelin J, Arganda-Carreras I, Frise E, Kaynig V, Longair M, Pietzsch T, Preibisch S, Rueden C, Saalfeld S, Schmid B, et al. (2012). Fiji: an open-source platform for biological-image analysis. Nature methods 9, 676–682. [PubMed: 22743772]
55. Peirce JW (2007). PsychoPy--Psychophysics software in Python. Journal of neuroscience methods 162, 8–13. [PubMed: 17254636]
56. Rose T, Jaepel J, Hubener M, and Bonhoeffer T (2016). Cell-specific restoration of stimulus preference after monocular deprivation in the visual cortex. Science 352, 1319–1322. [PubMed: 27284193]
57. Baker CA, Elyada YM, Parra A, and Bolton MM (2016). Cellular resolution circuit mapping with temporal-focused excitation of soma-targeted channelrhodopsin. eLife 5.
58. Berens P (2009). CircStat: A MATLAB Toolbox for Circular Statistics. 2009 31, 21.

Highlights

- Tree shrews learn to make fine visual discriminations of stimulus orientation.
- Learning is accompanied by enhanced discrimination capacity in V1 neurons.
- Enhancement is linked to changes in tuning properties of task-relevant neurons.
- Persistence of these changes leads to predictable biases in behavioral performance.

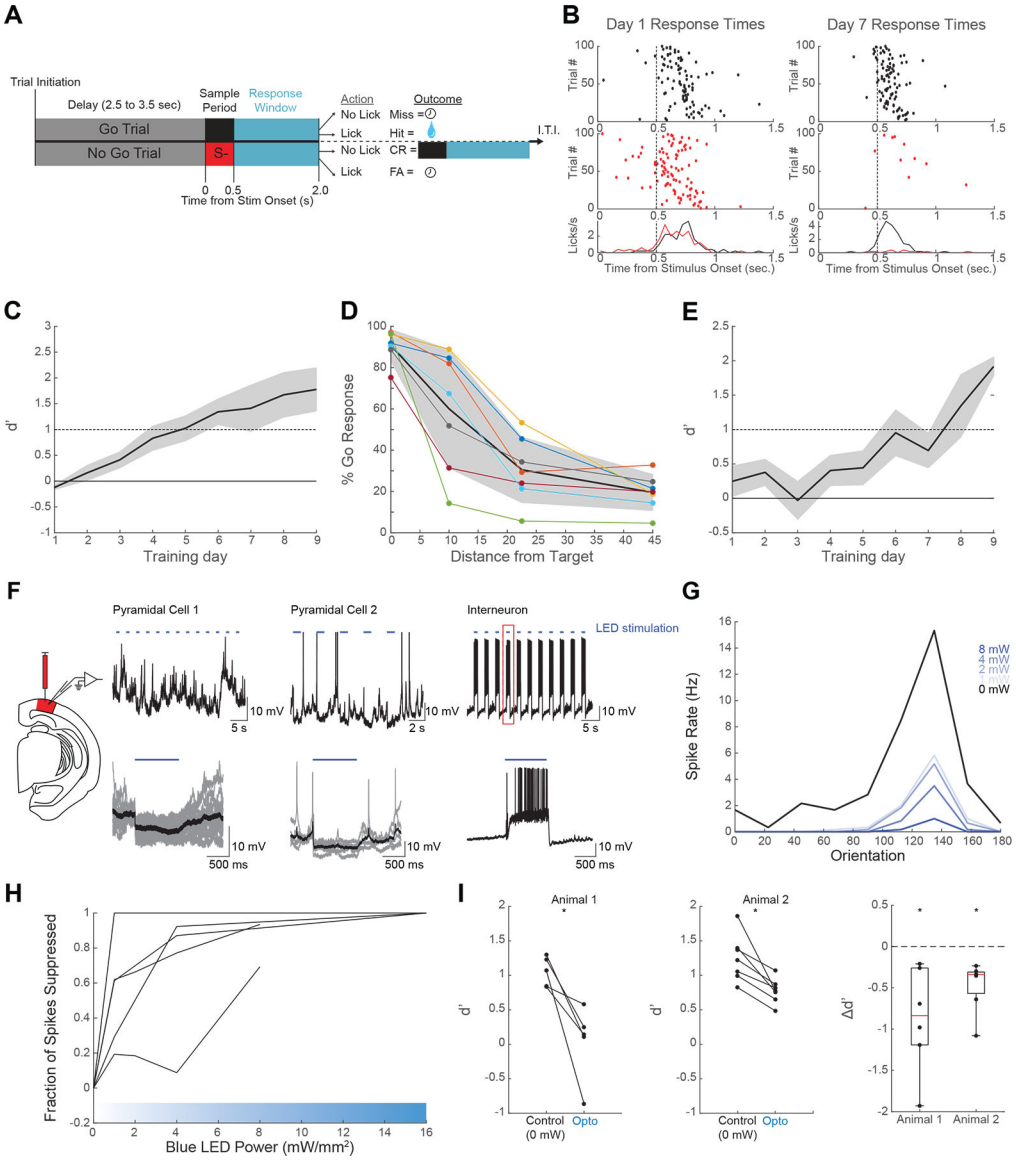

Figure 1: Tree shrews learn to perform a V1-dependent orientation discrimination task.

(A) Task structure. Tree shrews self-initiated trials by licking their response port. Following a variable delay, shrews were asked to lick following an S+ orientation while not licking in response to an S− orientation. Hit trials elicited liquid rewards, while correct rejections (CR) resulted in a subsequent S+ presentation. Miss and false alarm (FA) trials resulted in a brief time-out. Inter-trial interval (ITI) was determined by the tree shrew. **(B)** Representative performance for days 1 (left) and 7 (right) demonstrates coarse discrimination learning. The tree shrew initially licks indiscriminately for both S+ (black) and S− (red) trials. After one week of training the shrew licks predominantly on S+ trials, while rejecting S− trials. Lick time histograms (bottom) show a refinement of response times to immediately follow the stimulus presentation on day 7. **(C)** Mean (+/− SEM) performance showing shrews on average reached criterion performance within one week of training (n = 11; mean days to criterion = 6.17 +/− 2.92 SD) **(D)** 7 shrews were trained to perform the task with multiple

S− offsets. Performance at 10 degree discriminations was unreliable, while shrews were able to achieve reliable suppression of go responses for S− orientations of 22.5 degrees or higher. **(E)** Mean (+/− SEM) learning curves show fine discriminations of 22.5 degrees reached criterion levels on average after 7.44 days of training (+/− 3.0) **(F)** Expression of ChR2 under the mdlx enhancer in V1 enabled blue-light mediated suppression in two example pyramidal neurons (top: raw whole-cell voltage recordings; bottom: individual stimulus locked trials in grey, with average traces in black). Fast-spiking excitation was observed in a putative interneuron (top: raw whole-cell trace; bottom: example stimulus locked trial outlined in red above). **(G)** Orientation tuning curves recorded at varying levels of blue light power from one example neuron show increasing spike suppression across orientations. **(H)** 5 neurons showed increasing spike suppression at preferred orientation with as little as 1mW/mm2 **(I)** 2 headfixed shrews were implanted with bilateral windows over V1 expressing ChR2 via the mdlx enhancer. Average discrimination performance was impaired during trials with optogenetic stimulation in both animals. The left two panels show discrimination performance decrements for individual sessions. The right panel shows Δd’ distributions for each animal (*p<0.01 Wilcoxon signed rank test). See also Figure S1.

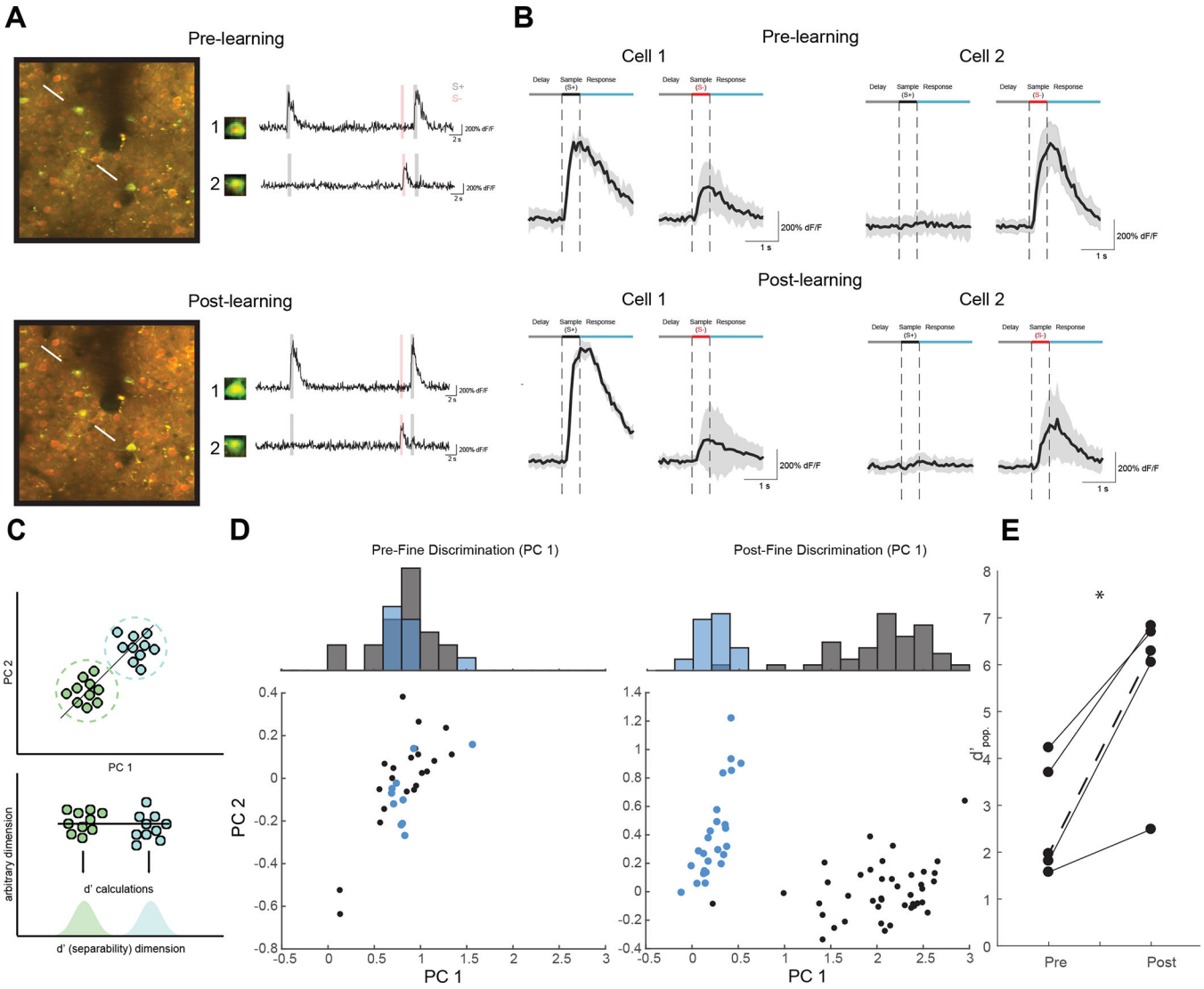

Figure 2: Tracking neural populations over the time reveals learning-related enhancement of neural population discrimination.

(A) Neural response properties were measured at pre- (top) and post-learning (bottom) time points during learning. The neurons within the same field of view were identified across sessions. Example neural response traces for tracked cell bodies are shown as raw dF/F traces (right). **(B)** Mean stimulus locked traces (+/− SEM) for example neurons in a.. Cell 1 was an S+ selective cell that became more selective over time. Cell 2 was an S− selective cell that became less selective over time. See also Figure S2 **(C)** Schematic of neural population discrimination. Individual population responses are color coded by stimuli and plotted by their first 2 principle components (top). Each data point (individual trial) was then projected onto the vector connecting the mean response to each stimulus, and d' measures were computed via the 1-d projection distributions (bottom) **(D)** Population responses for an example animal before and after learning in neural discrimination space (bottom) and marginal histogram (top). Pre-learning (left) the S+ (Black) and 22.5 degree S− (blue) are highly overlapping. In the post-learning recording (right) the S+ is highly separable from the

S− distribution. (E) Five animals display a positive $\Delta d'_{pop.}$ between pre- and post-learning recordings (*p<0.05, paired t-test). The example animal from **D**. is shown as a dashed line.

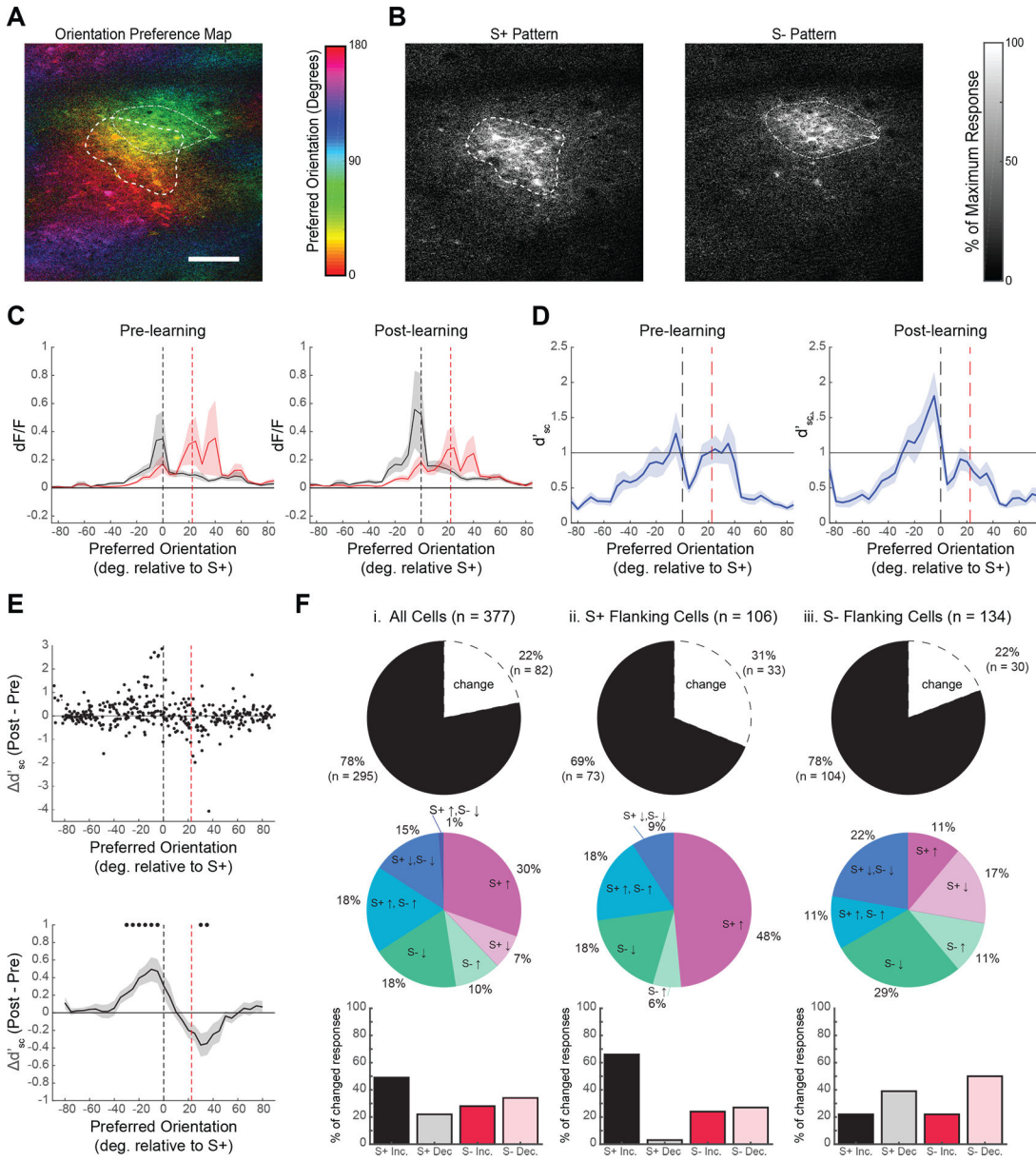

Figure 3. Single cell improvements in neural discrimination are predicted by baseline discrimination capacity and reward associations.

(A) Tree shrew V1 contains an orderly map of orientation preference. The orientation preference map is computed from responses to oriented gratings during passive viewing. **(B)** Average calcium responses to S+ (left) and S− (right) stimuli shown during behavior are distributed over overlapping columns within V1, with many of the same neurons responding for both stimuli. Contours outline cortical regions responding greater than 30% of the maximum response per stimulus, and are overlaid on the orientation map in a. **(C)** Population response curves from binned single cell responses (dF/F) to S+ (black) and S− (red) stimuli, arranged by preferred orientation for pre- (left) and post-learning (right) conditions. **(D)** Average binned single cell d' values arranged by each neuron's preferred orientation. Pre-learning (left), peak d' values were observed in neurons with preferred

orientations flanking the S+ and S− stimuli, and were lower in between the S+ and S−, indicating that these neurons provide minimal discrimination information for the task. Post-learning (right) a significant bias exists with S+ flanking neurons displaying greater discrimination information than S− flanking neurons. **(E)** Top: V1 neurons with the greatest learning related improvements in d'_{sc} have preferred orientations neighboring the S+ (black dashed line), but not S− stimulus (red dashed line). Significant increases in d'_{sc} were found up to 30 degrees from the S+ stimulus, while significant decreases in d'_{sc} was observed near the S− stimulus (bottom: averaging Δ d' over a moving window of preferred orientations in 5 degree increments with 20 degree bin size, mean +/− SEM, *$p<0.05$ Wilcoxon signed-rank test). **(F)** Learning related changes in responses to task-relevant stimuli depended largely on the functional properties of neurons relative to the orientations of the task. Top row: percentages of neurons with a significant change ($p<0.05$, Wilcoxon Signed-rank test) in the magnitude of response to at least one task relevant stimulus out of i. all cells (22%), ii. S+ flanking cells (31%), and iii. S− flanking cells (22%). Middle row: breakdown in specific types of statistically significant changes observed on a cell by cell basis. Out of all cells and S− flanking cells there were heterogenous changes in the magnitude of responses to both stimuli, while S+ flanking cells largely saw increases in S+ responses. Bottom row: total proportions of significantly changing cells exhibiting increases or decreases in response to the S+ or S−. S+ flanking cells are heavily dominated by increases in response to the S+ (66%), while S− flanking neurons show balanced changes with S− decreases being the prevailing change (51%). See also Figures S3 and S4.

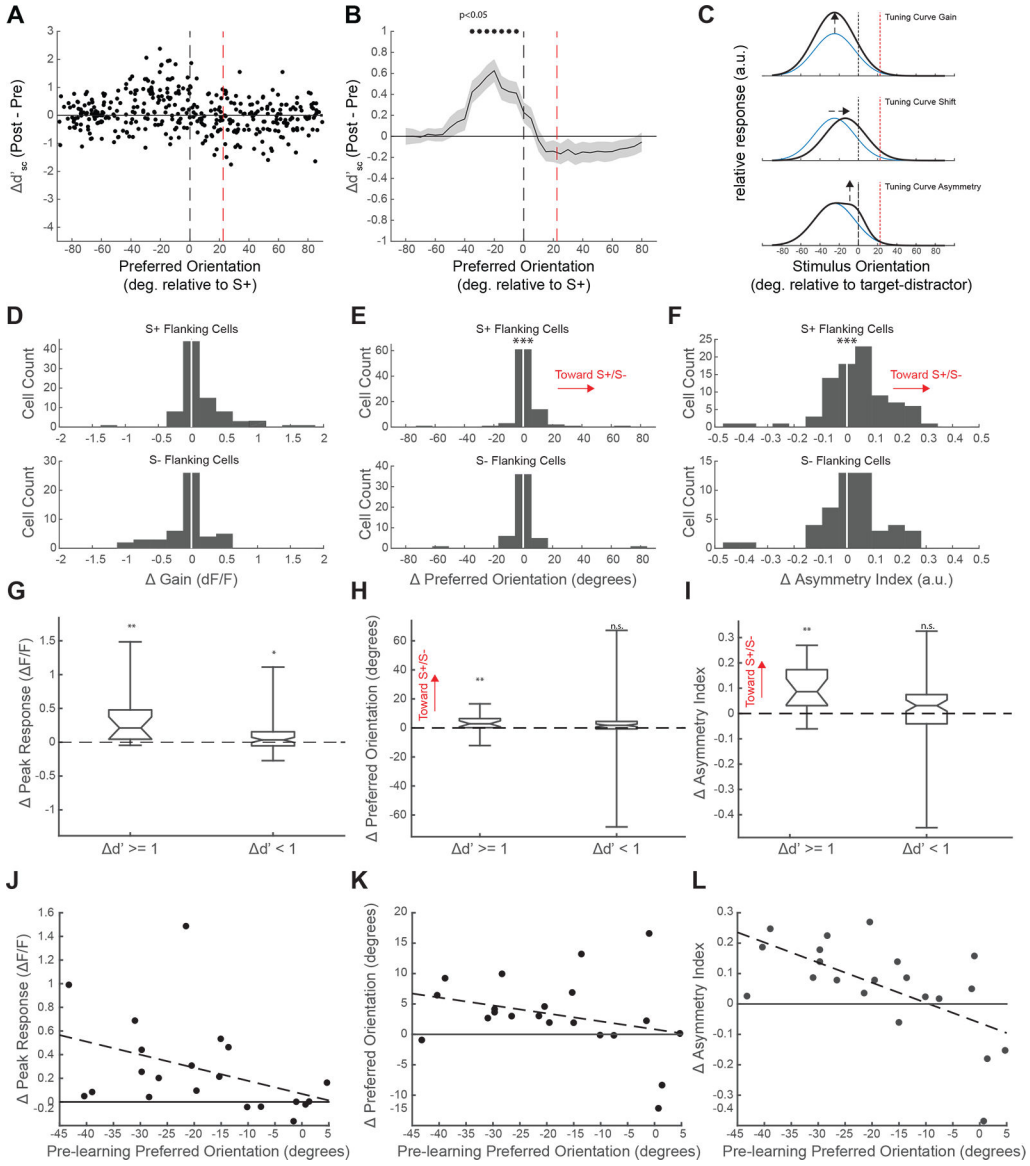

Figure 4. Single cell improvements in neural discrimination persist during passive stimulus presentations and are consistent with biased shifts in preferred orientation.

(A) As in Figure 3E, single V1 cells with the greatest imcreases in passive d'$_{sc}$ had preferred orientations neighboring the S_, but not S− stimuli. **(B)** Significant increases in delta d'$_{sc}$ were found between 5 and 30 degrees from the S+ stimulus (averaging delta d' over a moving window of preferred orientations in 5 degree increments with a 20 degree bin size, mean +/− SEM, *p<0.05 Wilcoxon signed rank test with Bonferroni correction). **(C)** Three types of hypothetical functional changes leading to selectively increased d'$_{sc}$ in V1 neurons. Top: a positive gain in excitation of a single S+ flanking neuron. Middle: a small shift in preferred orientation toward the S+ orientation. Bottom: an asymmetrically biased increase in excitation in the vicinity of the S+ orientation **(D)** S+ flanking cells (Top) but not S− flanking cells (Bottom) exhibit a gain in response magnitude (***P<0.001 Wilcoxon signed rank test). **(E)** S+ flanking cells (Top) but not S− flanking cells (Bottom) exhibit a biased shift in their orientation preference with learning (***P<0.001, Wilcoxon signed rank test).

(F) S+ flanking cells (Top) but not S− flanking cells (Bottom) exhibit an overall positive shift in their Asymmetry index with learning (***P<0.001, Wilcoxon signed rank test). **(G)** Neurons in the S+ flanking domain with high and low increases d' exhibited significant gains in response magnitude (*p<0.05, **p<0.01, Wilcoxon signed rank test). **(H)** Only S+ flanking neurons with high increases in d' exhibited significant positive shifts in preferred orientation (**p<0.01 Wilcoxon signed rank test). **(I)** Only S+ flanking neurons with high increases in d' exhibited significant positive shifts in asymmetry index (**p<0.01 Wilcoxon signed rank test). **(J)** Out of the subpopulation of S+ flanking neurons with high increases in d', pre-learning orientation preference was not significantly correlated with chang in the magnitude of neuronal response (Linear regression, p>0.06, R-square = 0.17). **(K)** In the same neurons shown in **J**, pre learning preferred orientation was not significantly correlated with change in preferred orienatation (Linear regression, p=0.18, R-square = 0.08. **(L)** In the same neurons shown in **J** and **K**, pre-learning preferred orientation was significantly correlated with change in asymmetry index (Linear regression, p<0.01, R-square = 0.39). See also Figure S4.

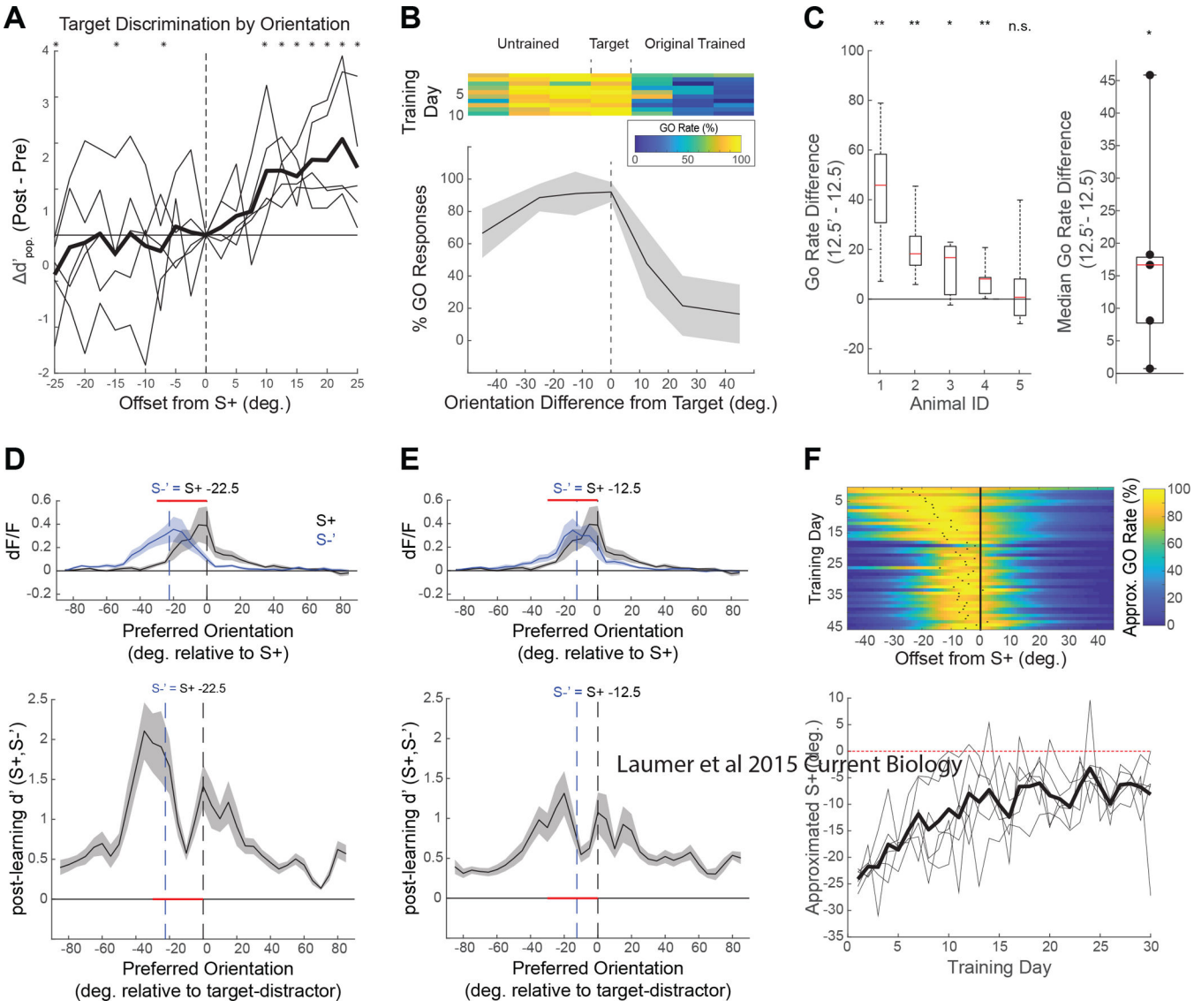

Figure 5. Tree shrew neural discrimination accurately predicts orientation specific benefits and impairments in future behavioral performance.

(A) Learning-related changes in d'$_{pop}$ of the S+ (0 degrees) and a wide range of passively viewed orientations further reveals the orientation specificity of the training effect. Average peak Δd'$_{pop}$ for population discrimination was seen at the 22.5 degrees (equal to the S−), with gradual increases in d' observed between the S+ and S−. While no average improvements in d'$_{pop}$ were observed for orientations on the other side of the S+, small but significant decreases in discrimination performance were seen in three of these untrained orientations (*p<0.05 Wilcoxon signed rank test). **(B)** Tree shrews that initially learned the original asymmetric discrimination were introduced to a generalized, symmetric discrimination task in which multiple S− stimuli were introduced on either side of the S+ orientation. 10 days of performance after tree shrews were introduced to a novel task shows that one example shrew was biased to go for novel orientations, but maintained accurate performance for the original discriminations (>= +22.5 degrees). **(C)** 4 out of 5

tree shrews showed significant transference of skill in discriminating the S+ from novel +12.5 orientation compared to the novel −12.5 S− orientation (Left: **p<0.01, *p<0.05, Wilcoxon signed rank test; Animal 1 is the example in **B**). Across animals (right), median go rates were higher for the −12.5 degree compared to the +12.5 degree S− stimulus (p<0.05, Wilcoxon signed rank test). **(Top D, E)** Passively recorded population response curves (as in **3C**) for the S+ (black) and a hypothetical novel S− (**D**: −22.5; **E**: −12.5; blue) after shrews were trained on the original fine discrimination. Regions of the population that are enhanced through reward association (red) overlap with the regions of the population that respond robustly to both the S+ and novel S− **(Bottom D, E)** Average post learning d' for the novel S−' and original S+ arranged by preferred orientation. Regions with poor discrimination are overlapping with the subpopulation of neurons that are enhanced through reward association for the original task, predicting that the learning of this novel discrimination should be impaired following learning of the original fine discrimination task. **(F)** Gaussian curves were fit to each day's psychometric function (see 5B) and tracked for at least 30 days. The peak of the Gaussian is taken as an approximation for the orientation at which the shrew exhibits it's peak go rate, and thus represents the orientation at which the shrews exhibit minimal discrimination from the S+. Over 30 days of behavioral training, shrews maintain a persistent impairment in discriminating stimuli on the novel side of the S+, and on average continue to associate stimuli within approximately 10 degrees of the S+ with a go response.

KEY RESOURCES TABLE

REAGENT or RESOURCE	SOURCE	IDENTIFIER
Bacterial and virus strains		
AAV9-Syn.GCaMP6s.WPRE.SV40	UPenn Vector Core; Addgene	RRID:Addgene_100843
AAV1-hSyn1-mRuby2-GSG-P2A-GCaMP6s-WPRE-pA	Addgene	RRID:Addgene_50942
AAV9-mDlx-ChR2-mCherry-Fishell-3	Addgene; Vigene	RRID:Addgene_83898
AAV2/1.mDlx.ChR2-FLAG-Kv2.1.p2a.H2b-CyRFP	Max Planck Florida Institute for Neuroscience; Vigene	N/A
Experimental models: Organisms/strains		
Tree shrews (Tupaia belangeri)	Max Planck Florida Institute for Neuroscience	N/A
Deposited data		
Two-photon calcium imaging and behavior dataset	This paper	https://doi.org/10.7910/DVN/O1CHOV
Software and algorithms		
Scanimage 2015, 2018	Vidrio Technologies	RRID:SCR_014307
MATLAB 2015,2017,2018a	Mathworks	RRID:SCR_001622
ImageJ (Fiji)	Schindelin et al. (2012)[54]	RRID:SCR_002285
Python 2.7, 3.6	Python Software Foundation	RRID:SCR_008394
PsychoPy	Peirce et al. 2007[55]	RRID:SCR_006571
LabVIEW	National Instruments	RRID:SCR_014325
Spike2	Cambridge Electronic Design	RRID:SCR_000903
Custom MATLAB and Python scripts for analysis and experimental control	This Paper	https:/github.com/joschumacher